Chapter 5

Airborne Magnetic Surveys to Investigate High Temperature Geothermal Reservoirs

Supri Soengkono

Additional information is available at the end of the chapter

http://dx.doi.org/10.5772/61651

Abstract

Airborne magnetic survey is an effective geophysical exploration method in terms of coverage, resolution and cost, particularly for area with restricted or difficult ground access. Research studies in New Zealand have shown airborne magnetic surveys can indicate the regions of high reservoir permeability and thermal up-flow of active geothermal systems. However, the method has not been extensively used in the geothermal investigations, probably because the interpretation of airborne magnetic data has so far been seen as difficult and requires a complex quantitative 3D modelling of subsurface magnetisation.

This chapter introduces a new approach to use airborne magnetic survey to investigate high temperature geothermal resources without the need of 3D magnetic modelling. This new approach takes advantage of data processing packages that during the last few years have become accessible through the internet. A simple but comprehensive explanation is given on the physics background of the airborne magnetic surveys. Examples are provided from interpretations of real airborne magnetic data from the North Island of New Zealand and the Java Island of Indonesia. This chapter is aimed to provide the readers a sufficient level of knowledge and confidence to organise and/or run investigation of high temperature geothermal reservoirs using airborne magnetic surveys.

Keywords: Total force magnetic anomalies, magnetisation of volcanic rocks, hydrothermal alteration and demagnetisation, extent of geothermal reservoirs, reversely magnetised rocks

1. Introduction

Airborne magnetic survey involves measurements of the geomagnetic field (the magnetic field of the earth) from the air using magnetometer installed in an aircraft. The purpose is to detect small changes in the geomagnetic field related to differences in rock magnetisation beneath

the survey area. The airborne magnetic survey has been extensively applied in the mineral explorations and as additional tool to support geological mapping projects. It is a very effective geophysical exploration technique in terms of coverage, resolution and cost, particularly in area with difficult or restricted ground access. The airborne magnetic surveys over the Taupo Volcanic Zone (TVZ) in New Zealand, which started with a regional survey dating back more than 60 years ago in the early 1950s [9] and was followed in much later date by a variety of more detailed surveys between 1984 and 2006 [24,14,31], have provided data sets that all are highly consistent to each other. The resolution of the dataset, as expected, depends on the flight line spacing and the survey altitude above the ground. But all the data sets revealed the same features of magnetic anomalies. This consistency clearly shows that airborne magnetic survey is a robust geophysical method. Over geothermal prospect regions worldwide, airborne magnetic data are often already available from some previously conducted surveys by mineral exploration companies searching for epithermal gold deposits or by the government institutions (Geological Surveys).

Hochstein and Soengkono [14] showed that careful interpretations and three dimensional (3D) quantitative modelling of airborne magnetic anomalies over many geothermal systems in the Taupo Volcanic Zone (TVZ) in New Zealand can provide information on the likely locations of high reservoir permeability and up-flow regions of active geothermal system. They also quoted examples that suggest this would also likely be true for geothermal systems in volcanic settings elsewhere outside New Zealand. However, the interest to use data from airborne magnetic surveys to investigate high temperature geothermal systems has been very slow to develop. A possible reason of this slow development is that the interpretation of magnetic data in geothermal investigations has been considered difficult and the 3D quantitative modelling of the magnetic data can be a complex and problematic task. The changing in geomagnetic inclination at different geographic latitudes causes different pattern of magnetic anomalies over areas which have the same geological structures and lithology but are located at different geographic regions. In addition, unlike the scalar parameter rock density that causes gravity anomalies, the rock magnetisation is a vector. Because of this, the pattern of the magnetic anomalies is complex and more difficult to interpret than the gravity anomalies over the same area. However, with the development of user friendly geophysical processing packages that, since mid-2000s, have become accessible on-line (worldwide), the complexity of magnetic anomalies can now be reduced.

This chapter introduces and explains a new approach to use airborne magnetic data for the investigations of high temperature geothermal resources hosted by volcanic rocks. This new approach is specifically formulated for this chapter based upon the author's experience during the last 30 years in the interpretation and 3D modelling of various airborne magnetic data. It has not been previously published in any papers listed in the reference list of this chapter (Section 7), nor anywhere else. This approach utilises some magnetic data processing techniques in the computer software that have now become accessible worldwide. The processing techniques are used to directly link the measured airborne magnetic anomalies to the causative source targets. The often complex and difficult 3D modelling of the anomalies would only need to be carried out when it is considered necessary at the final stage of the interpretation, when

http://dx.doi.org/10.5772/61651

some further detailed aspects of the magnetic interpretation need to be pursued. The aim of this chapter is to equip readers with some knowledge and confidence to run the investigation of high temperature geothermal reservoirs in volcanic rocks using airborne magnetic data which are already available over target area from some previous surveys, or going to be collected by a new survey specifically aimed to explore the geothermal targets.

The SI unit of magnetic field strength is Tesla, or T ($T=Weber/m^2=Vs/m^2$). The unit used for geomagnetic field strength measured during airborne magnetic survey is nT ($1\ nT = 10^{-9}T$), which is equal to the old unit gamma (γ) ($1nT = 1\gamma$).

2. The geomagnetic field

2.1. The normal geomagnetic field

The normal (undisturbed) geomagnetic field $\mathbf{B_o}$ can be approached by the effects of a fictitious magnetic dipole at the centre of the earth, orientating at a small angle (about 10°) to the axis of earth rotation. On the surface of the earth, the *inclination* of the normal geomagnetic field causes by such a dipole varies from +/-90° at the magnetic north and south poles, to 0° at the magnetic equator (see Figure 1). As the positions of the north and south magnetic (N' and S') and geographic (N and S) poles are not the same, there is also a horizontal *declination* between the magnetic north (the horizontal direction of the earth's magnetic field shown by a compass needle) and the geographic north. The magnetic inclination is considered positive downwards; it is negative in the southern hemisphere (such as in NZ, Australia and Africa). Since the fictitious dipole at the centre of the earth is only quasi static (it has a slow precession around the earth rotational axis), there is a small secular variation of the normal geomagnetic field.

Studies of *remanen*t magnetisation (the permanent magnetisation that is not induced by the present day geomagnetic field) of the rocks of different ages from around the earth show that the orientation of the fictitious dipole at the centre of the earth had flipped many times in the past, when the positions of N' and S' were interchanged (called the geomagnetic reversal). The last geomagnetic reversal occurred about 0.7 Myr ago [19].

The normal geomagnetic field of the earth ranges in strength from about 35,000 nT near the equator to about 60,000 nT near the north and south poles. For examples, in the North Island of New Zealand (about 38°S latitude) it has the strength of about 54,000 nT whereas in the Java Island of Indonesia (about 7°S latitude) the geomagnetic field strength is about 44,000 nT. At any point on the surface of the earth, the strength and direction (declination and inclination) of the normal geomagnetic field can be obtained from the internet (by searching for "geomagnetic field strength" to get to web sites to do the calculation online). The geomagnetic values are computed using a global model, defined by spherical harmonic coefficients synthesising the quasi static component as well as the secular variation of the earth's magnetic field, and is known as the International Geomagnetic Reference Field (IGRF). This global model is renewed every about 5 years by collaborative effort between magnetic field modellers and the institutes involved in collecting and disseminating magnetic field data from satellites and from observ-

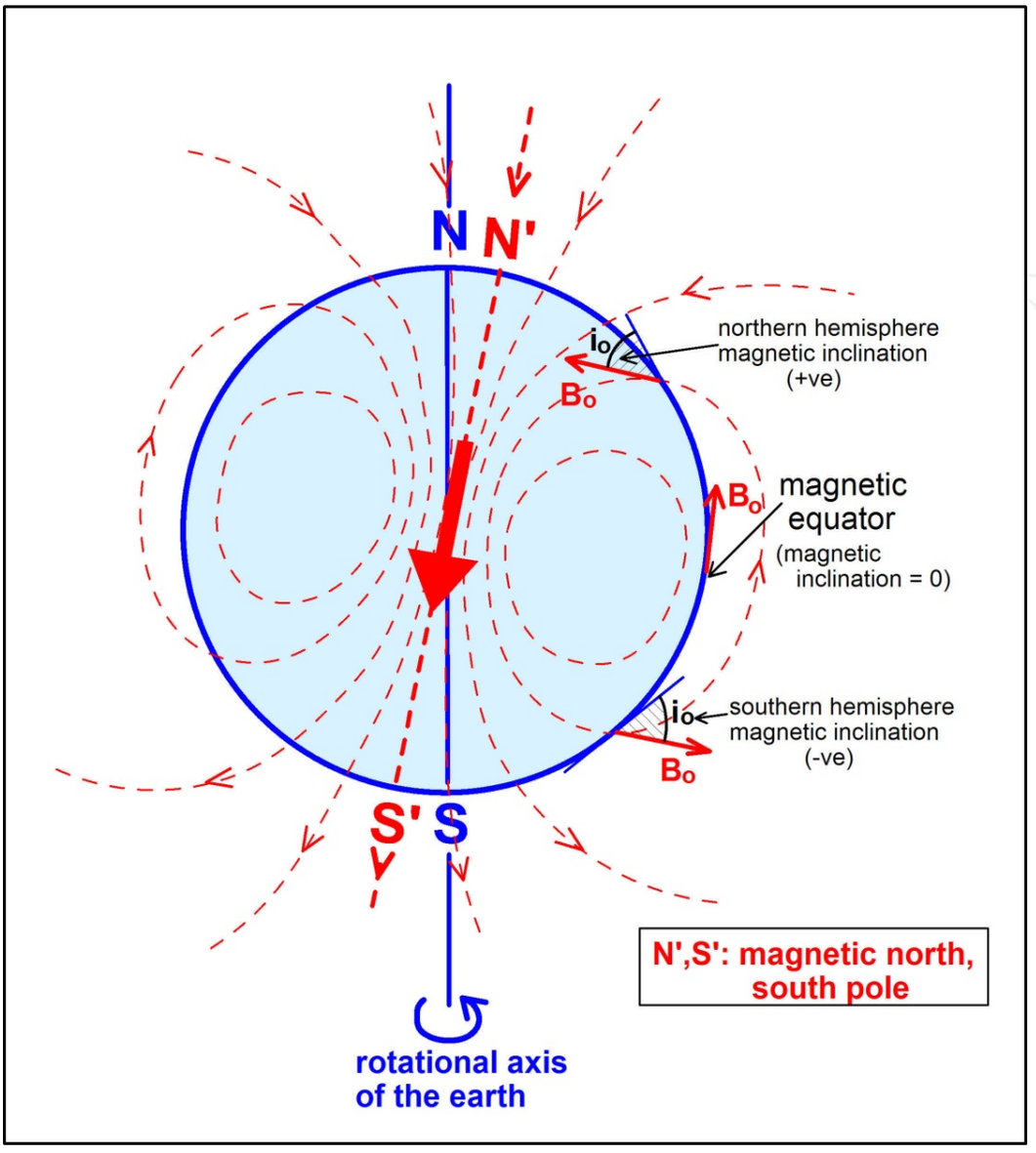

Figure 1. The normal geomagnetic field of the earth.

atories and surveys around the world. Note that the value of the magnetic inclination is not the same as the value of geographical latitude.

2.2. Diurnal variations

The total geomagnetic field measured during a magnetic survey contains small magnetic fields related to local variation of rock magnetisation (this is the target of airborne magnetic survey) and time variant external components from outside the solid earth. The time variant external field includes small diurnal variations (range about 30 nT) of about 24 hours period which correlate with electrical currents in the ionosphere, and a larger transient and erratic disturbance (range up to 1000 nT) known as magnetic storms which correlate with sunspot activity. The effect of the time variant external fields has to be corrected from the measured airborne

http://dx.doi.org/10.5772/61651

magnetic data. If magnetic storm is avoided when conducting the survey, the only significant time variant field affecting the measured geomagnetic field would be that causing the diurnal variations. Near the earth's surface, the magnetic field causing the diurnal variations has an almost constant strength and direction within a 75 km radius. For a magnetic survey it is therefore sufficient to monitor the diurnal variations at a base station within or near the survey area. Data provided by airborne magnetic survey companies contracted to carry out the survey would have been corrected for this diurnal variation.

2.3. Magnetic anomalies

Figure 2 shows a schematic vector diagram of the relationship between total geomagnetic field ($\mathbf{B_{obs}}$), the normal (undisturbed) geomagnetic field ($\mathbf{B_o}$) and the total sum of local magnetic fields produced by variations of rock magnetisation ($\mathbf{\Delta B}$), at two theoretical measurement points (a) and (b) having two different $\mathbf{\Delta B}$ vectors. The strength of total geomagnetic field vector ($=|\mathbf{B_{obs}}|$) is the *only* parameter measured during airborne magnetic survey. As shown in Figure 2, this measured geomagnetic magnetic field $\mathbf{B_{obs}}$ vector is the result of vector operation $\mathbf{B_{obs}} = \mathbf{B_o} + \mathbf{\Delta B}$. The sum magnetic field strength caused by anomalous bodies ($|\Delta B|$) is usually much smaller (less than 2%) compared to the strength of the normal geomagnetic field ($|\mathbf{B_o}|$) (except at a ground location close to an outcrop of very highly magnetic rocks). Hence, the angle between $\mathbf{B_o}$ and $\mathbf{B_{obs}}$ is very small (less than 2°).

The *total force magnetic anomaly* (termed in this chapter as ΔF) is defined by algebraic (scalar) subtraction of $|\mathbf{B_o}|$ (the strength "undisturbed" earth's magnetic field) from $|\mathbf{B_{obs}}|$, that is: $\Delta F = |\mathbf{B_{obs}}| - |\mathbf{B_o}|$. As $|\mathbf{B_o}|$ cannot (are not) directly measured, the value $|\mathbf{B_o}|$ it is usually taken from computation of the IGRF (see Section 2). The ΔF computed from the measured $|\mathbf{B_{obs}}|$ subtracted by the IGRF value contains all the magnetically anomalous mass beneath the measurement point down to very deep level (theoretically it is down to the depth of the fictitious magnetic dipole near the centre of the earth). To approximate ΔF affected only by magnetically anomalous mass beneath the "survey target", one can use the trend of $|\mathbf{B_{obs}}|$ across the survey area to determine $|\mathbf{B_o}|$**.** No exact value of such survey target "depth" can be given, but the ΔF values obtained in this way are better for identifying and delineating the survey target. For this reason, computer software that can properly grid airborne magnetic data and compute the trend of gridded data is essential in the interpretation of airborne magnetic surveys. The computation of trends and other processing and plotting of the magnetic data presented in this chapter are all carried out using the computer software Oasis Montaj from the Geosoft Inc. There are some other software packages available in the market (can be purchased online) that can do the same processing and plotting.

If the airborne magnetic data that available for the investigation are already in the form of ΔF obtained by subtracting of the IGRF values (often this is the case with data received from the airborne magnetic survey contractor), removing the trend of such ΔF values over the survey area will provide new (corrected) ΔF values that would represent magnetically anomalous bodies no deeper than the "survey target".

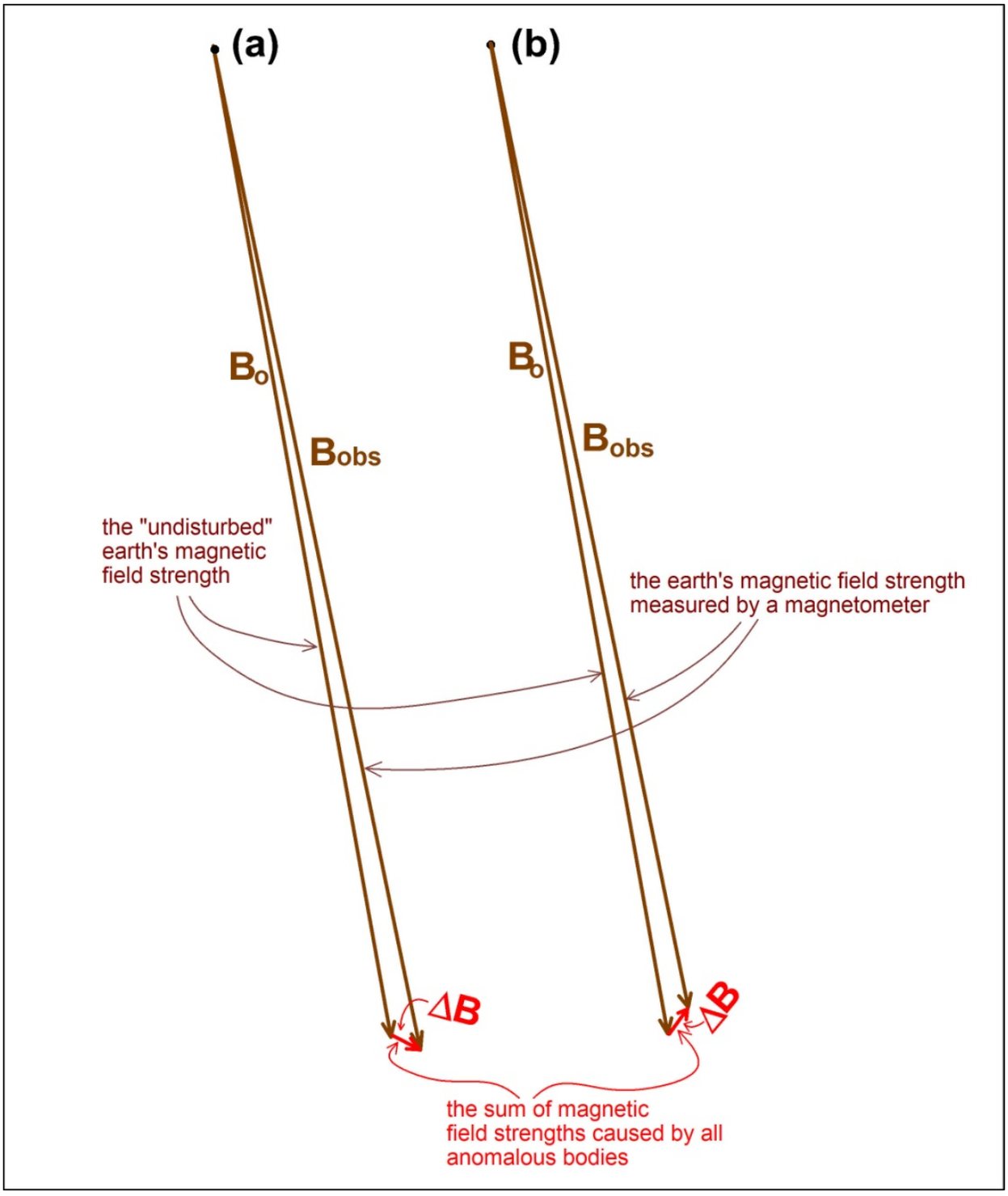

Figure 2. Vector diagram of magnetic anomalies. In (a) **ΔB** adds to $\mathbf{B}_o$ and we obtain positive total force magnetic anomaly ΔF. In (b) **ΔB** opposes $\mathbf{B}_o$ and the total force magnetic anomaly is negative.

http://dx.doi.org/10.5772/61651

2.4. The patterns of a magnetic anomalies caused by magnetic dipole

First order effects of observed magnetic anomalies can often be interpreted by simple dipole fields (such field are set up by geological bodies that can be approximated by a magnetic dipole or combination of dipoles). This is especially true for geological bodies that can be approximated by a homogeneous sphere, since homogeneous sphere is magnetically equivalent to a single magnetic dipole placed at its centre.

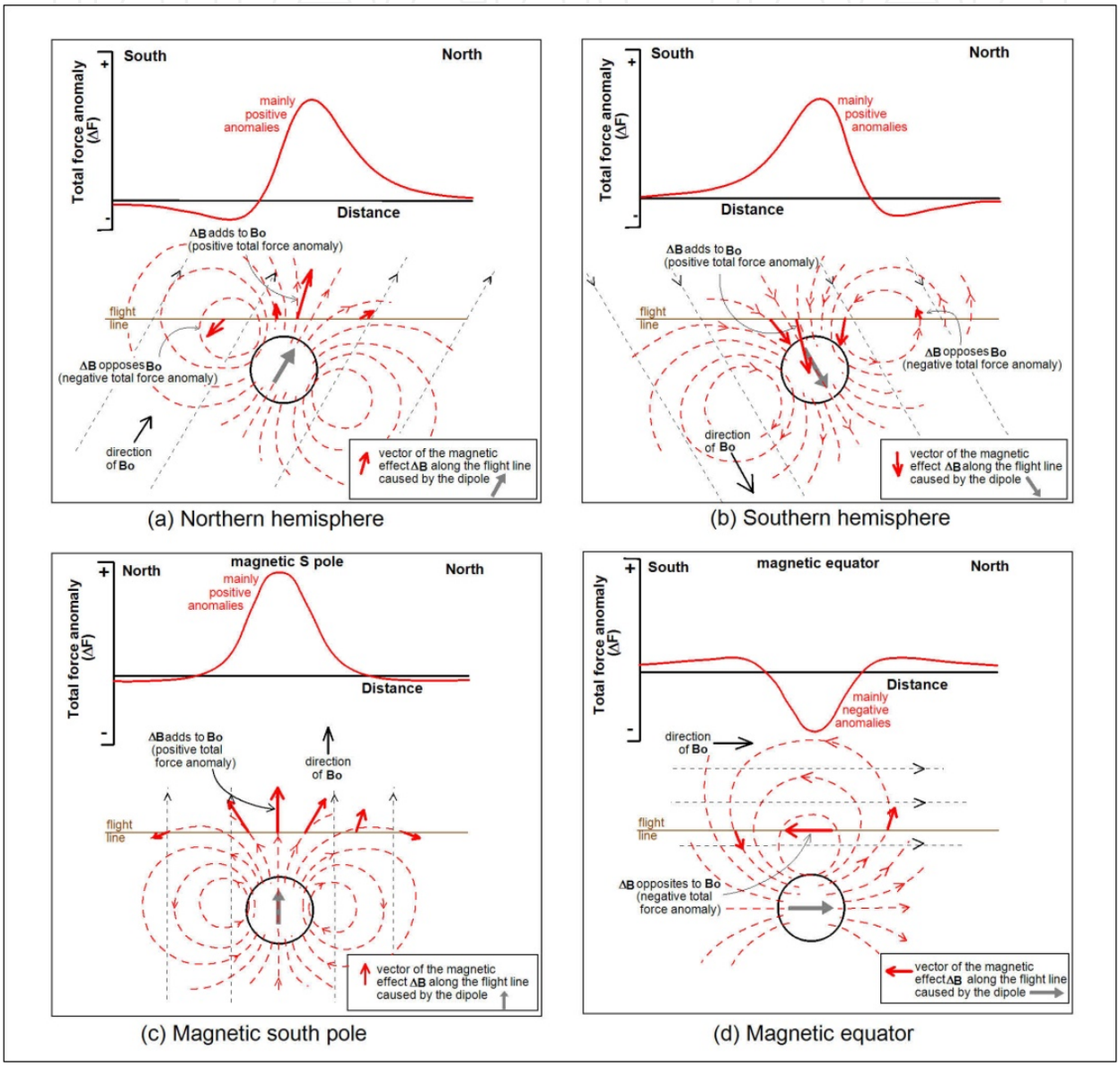

Figure 3. Total force magnetic anomalies caused by a magnetic dipole (or a magnetic sphere) at different geomagnetic inclination (different geographic latitudes).

Figure 3 shows diagrams explaining the patterns of total force anomalies (ΔF) caused by *positive* magnetic dipoles (orientated in *the same direction* as $\mathbf{B}_o$) that are located in: (a) the northern hemisphere, (b) the southern hemisphere, (c) the magnetic *south* pole and (d) the magnetic

equator. For the magnetic *north* pole, by using a diagram equivalent to Figure 3 (c) but with a vertical downward direction of the magnetic dipole and $\mathbf{B}_o$, it can easily be shown that the pattern of the created total force anomaly (ΔF) is exactly the same as that shown in Figure 3 (c). The same can be made also for *negative* magnetic dipoles (orientated *opposite in direction* to $\mathbf{B}_o$), which will show the patterns of total force anomalies in Figure 3, but with ΔF values having the opposite sign. Figure 3 also shows that total force magnetic anomalies ΔF created by the *positive* magnetic dipoles at locations away from the magnetic equator are dominantly *positive*. At the south (or north) magnetic pole (Figure 3(c)), the centre of positive anomalies is located directly above the dipole. At the southern hemisphere (Figure 3(a)) the centre of the positive anomaly is shifted to the north of the magnetic dipole and at the northern hemisphere (Figure 3(b)) it is shifted to the south of the magnetic dipole. However, the opposite occurs at the locations close (within about ±10°) to the magnetic equator. Here, the magnetic anomalies created by a *positive* magnetic dipole become dominantly *negative*! This "counter intuitive" phenomenon can result in a serious error in the interpretations of magnetic anomalies at locations within about ±10° magnetic latitude as at some parts of Africa, South America and the southern part of the Philippines.

3. Interpretation of magnetic anomalies over geothermal areas

3.1. Magnetic anomalies over the Taupo Volcanic Zone (TVZ) in New Zealand

The Taupo Volcanic Zone (TVZ) is a region of Quaternary volcanic and geothermal activity in the central North Island of New Zealand. Almost all high temperature geothermal systems in New Zealand are located in this zone. As mentioned in the introduction, a regional airborne magnetic survey was conducted over the TVZ during early 1950s and it was followed much later on by more detailed surveys between 1984 and 2006. The geomagnetic field inclination in the TVZ is about -62.5°. Because of this high inclination, the relationship between magnetic anomalies and geological features is easier to recognise than in the regions with lower magnetic inclination. The phenomenon that distinct magnetic anomalies are often associated with geothermal reservoirs in the TVZ has been recognised more than 70 years ago by Watson-Munro [35]. However, in the regional map drawn using the data from the early 1950s regional survey (for example, Hunt and Whiteford [16]) the relationship between some geothermal fields and the magnetic anomalies is not obvious and can just be barely seen because of wide flight line spacing (2.5 km) of the survey. The interest in using magnetic surveys as an exploration tool declined in New Zealand in the 1960s when electrical methods were found to be more effective in delineating the lateral extent of conductive reservoir rocks.

The interest was revived when the Geothermal Institute (University of Auckland, New Zealand) started new, lower-level airborne magnetic surveys in 1984. One of the first surveys led to the discovery of a distinct magnetic anomaly over the Mokai geothermal field [20] that was hardly recognisable in the low resolution early map from the early 1950s survey. Between 1984 and late 1999s, the Geothermal Institute expanded the survey to cover an area of about 3000 km^2, covering all geothermal fields in the TVZ. Quantitative interpretation of more than

http://dx.doi.org/10.5772/61651

10 geothermal prospects within the area were undertaken [20,14,12-13,26-27,22-23,28-29,21,25,15]. The quantitative 3D interpretations indicated that airborne magnetic survey can be a useful tool to identify zone of high permeability region of an active geothermal system.

3.2. Magnetisation volcanic rocks

All volcanic rocks were magnetic after their eruption, as a result of their induced magnetisation ($\mathbf{m_i}$) and remanent magnetisation ($\mathbf{m_r}$). Remanent magnetisation is the permanent magnetisation of rock which was attained when the rock was formed (or deformed). The main type of remanent magnetisation in volcanic rocks such as lavas and ignimbrites is the thermo remanent magnetisation (TRM) which was attained when the rocks cooled down to below the Curie point of magnetite (about 580 ˚C). It has the same direction as the past $\mathbf{B_o}$ during the time of cooling. Induced magnetisation is given by the multiplication product of the geomagnetic field magnetising force **H** (A/m) and the magnetic susceptibility κ (a dimensionless parameter) which, in turn, is related mainly to the volume fraction of two primary magnetic minerals, magnetite and titanomagnetite. In the SI unit, the earth's magnetising force **H** can be determined from the relationship $\mathbf{B_o} = \mu H$, where μ is the magnetic permeability of the medium. For non-magnetic medium (such as air) $\mu = 4\pi \times 10^{-7}$ In the magnetic survey, the unit of $\mathbf{B_o}$ is nT (=10^{-9}T). Thus, H (in A/m) can be obtained from $\mathbf{B_o}$ (in nT) from $H=(1/\mu)\mathbf{B_o}.= (10^{-9}/(4\pi \times 10^{-7}))\mathbf{B_o} = 7.96 \times 10^{-4}\mathbf{B_o} \approx 8 \times 10^{-4}\mathbf{B_o}$ Hence, the induced magnetisation is given by the equation: $\mathbf{m_i} = \kappa\mathbf{H} = \kappa(8 \times 10^{-4})\mathbf{B_o}$. $\mathbf{m_i}$ has the same direction as the present day B_o.

In the TVZ, the strength of the induced magnetisation ($|\mathbf{m_i}|$) of rhyolites and ignimbrites is of the order of 0.5 A/m [21], pointing to the presence of about 0.8% (by volume) of primary magnetic minerals [17]. Petrology studies by Ewart [8] indicate magnetite values between 0.3 and 0.8% from "point counting". The strength of the remanent magnetisation ($|\mathbf{m_r}|$) of these rocks is significantly greater and lies commonly within the range of 1-4 A/m [21]. The strength of the total magnetisation ($\mathbf{m_t} = \mathbf{m_r} + \mathbf{m_i}$) of unaltered, normally magnetised volcanic rocks in the TVZ lies between about 0.5 A/m (tuffs, pumice, and volcanic breccia) and about 2.5 A/m (rhyolite lavas) [14]. The values cited are median values obtained from more than 200 rock samples measured by students at the Geothermal Institute (University of Auckland) between 1988 and 1993. The effect of an overprinted events associated with the natural fluctuation of geomagnetic field (known as the viscous remanent magnetisation, or VRM) in young rocks such as Quaternary volcanic rocks is likely to be small and can be neglected.

3.3. Hydrothermal demagnetisation of volcanic rocks

Hydrothermal alteration usually causes a "de-magnetisation" of initially magnetic reservoir rocks. Hydrothermal demagnetisation causes *negative* magnetisation contrast. Petrology studies show that, in these reservoirs, primary (titano-) magnetite has been replaced by almost non-magnetic minerals such as pyrite, leucoxene, or hematite [32]. In New Zealand some petrology studies in the Geothermal Institute (University of Auckland) showed that in liquid-dominated systems (titano-) magnetite appears to be the first mineral replaced during thermal alteration; this also applies to many liquid dominated systems in the Philippines and Indonesia

(Prof P.R.L. Browne, pers. comm., 1994). Hydrothermal demagnetisation appears to also occur in exposed rhyolite domed near the margins of some TVZ geothermal systems [20,26]. It seems acidic condensate formed in shallow vapour zones can cause demagnetisation of volcanic rocks forming topographic highs.

The solubility of magnetite increases rapidly in aqueous solutions with decreasing pH values (pH < 6) and at temperatures below 200°C [4]. Magnetite is also unstable in volcanic rocks that are saturated with CO_2-rich, steam heated waters with a pH value of <6. These occur, for example, near the top and margins of the Ohaaki reservoir in the TVZ [11]. The waters are corrosive and have caused significant external corrosion to well casings. All cores from the cooler well at Ohaaki which discharged such fluid were nearly non-magnetic. Since cooler, CO_2-rich waters at the margin of a gas-rich field like Ohaaki can also occur outside its boundary, it is possible that non-magnetic rocks can extend beyond the boundary of such a field delineated by resistivity surveys. Magnetite can be stable in the deeper oxidising environment of the natural two-phase system of Olkaria (Kenya) and, in that reservoir, it is less affected by thermal alteration than all other primary phases except quartz (Prof P.R.L Browne, pers. comm. 1994); the same applies to host rocks of the El Tatio outflow in Northern Chile. Because of this, the airborne magnetic survey identifies only the upper part of the geothermal reservoir. Except in the situations where the ground water flows have very strong horizontal component (associated, for example, with steep overall topography) the deep geothermal reservoir would be located beneath the zone of intensive hydrothermal demagnetisation.

Hydrothermal activity can also produce, on a smaller scale, a "'re-magnetisation" when pyrrhotite is deposited, which occurs as a secondary mineral in some New Zealand geothermal reservoirs. Little is known about the formation of this hydrothermal, magnetic trace mineral, which often can be found near rocks containing organic matter. Its magnetic stability range is restricted by its low Curie temperature (about 320°C according to Butler [6]). A study by Browne and Ellis [5] showed that small amounts of pyrrhotite occur in about one third of the wells at Ohaaki geothermal field in the TVZ. Pyrrhotite has also been found in a few wells at two other TVZ geothermal fields, the Wairakei and Waiotapu geothermal fields [33]; it is usually confined to barren fissures, not dispersed. Some 1990s studies by students at the Geothermal Institute (University of Auckland) of cores from 11 wells at Ohaaki geothermal field indicate that the magnetic effect of this alteration mineral (if present) would be small. However, two cores from one well at Ohaaki field at about 800 and 1100 m depths, which showed up with significant magnetisation contain no magnetite but some pyrrhotite. Overall, however, it appeared that "re-magnetisation'" of reservoir rocks caused by pyrrhotite deposition is small and can be neglected.

3.4. Reversely magnetised volcanic rocks

Reversely magnetised volcanic rocks are rocks which have $\mathbf{M}_r$ pointing opposite to the direction of the present day earth magnetic field. These volcanic rocks have thermo remanent magnetisation (TRM) which opposed the present day geomagnetic field because they were deposited and cooled down to temperature below the Curie point of magnetite (about 580˚C) the time of geomagnetic reversal. As the last reversal of the earth magnetic field occurred about

http://dx.doi.org/10.5772/61651

0.7 Myrs ago (Section 2.1) some older Quaternary volcanic rocks would be reversely magnetised (the Quaternary age ranges from 1.6 Myrs ago to recent). In the TVZ the strength of the reversed $\mathbf{m}_r$ is always greater than that of the induced magnetisation $\mathbf{m}_i$ [28,10]. This phenomenon is probably also true in all other Quaternary volcanic zones elsewhere. As the results, the total magnetisation ($\mathbf{m}_t$), which is the rock parameter affecting airborne magnetic anomalies, of the reversely magnetised Quaternary volcanic rocks is opposite in direction to $\mathbf{B}_o$. Reversely magnetised rocks have *negative* magnetisation contrast, the same type of magnetisation contrast as that caused by hydrothermal demagnetisation.

4. The pattern of total force magnetic anomalies caused by hydrothermal demagnetisation in different geographic locations

4.1. Pattern of the total force magnetic anomalies

To understand the magnetic anomaly pattern caused by geothermal systems at different geographical positions, the total force magnetic anomalies (ΔF) of a simplified model geothermal system (contains subsurface hydrothermally demagnetised rocks, a hill and a valley) were computed using 3D quantitative magnetic modelling code written by Soengkono [21] based on the equations of Barnett [2]. The computations were made for the geothermal system sited at different geographical locations; at high, moderate and low magnetic inclinations, at the magnetic poles and along the magnetic equator. The simplified model of geothermal system and its total force magnetic anomalies at the various magnetic inclinations are shown in Figures 4, 5, 6 and 7.

As already mentioned in Section 3.3, the hydrothermally demagnetised rocks have a *negative magnetisation contrast* with respect to the surrounding volcanic rocks. It should be noted that the magnetic model in Figures 4(a), 5(a), 6(a) and 7(a) will be still exactly the same magnetically if the hydrothermally demagnetised rocks body is given a $|\mathbf{M}_t|$ of -1.7 a/m and the surrounding homogeneous volcanic rocks mass is given a magnetisation $|\mathbf{M}_t|$ of 0 A/m. This is true because the magnetic effect of a one-dimensional magnetic body (a horizontal magnetic plate, or slab) is everywhere equal zero.

4.1.1. In the high magnetic inclination

Figure 4 shows the total force anomalies created by the simplified magnetic model at the southern hemisphere at geomagnetic inclination of -60° (Figure 4(b)) and at northern hemisphere at geomagnetic inclination of +60° (Figure 4(c)). In both Figures 4(b) and 4(c), the negative magnetisation contrast of the hydrothermally demagnetised rocks (the geothermal reservoir) causes bipolar total force magnetic anomaly with a dominant *magnetic low* (negative anomalies) that are easily recognised on the maps. Although the centre of the magnetic low is shifted from the entre of demagnetised rocks, the magnetic low can still clearly identify the demagnetised body. The extent of the magnetic low can be used almost directly to approximate (roughly delineate) the edges of the demagnetised rocks.

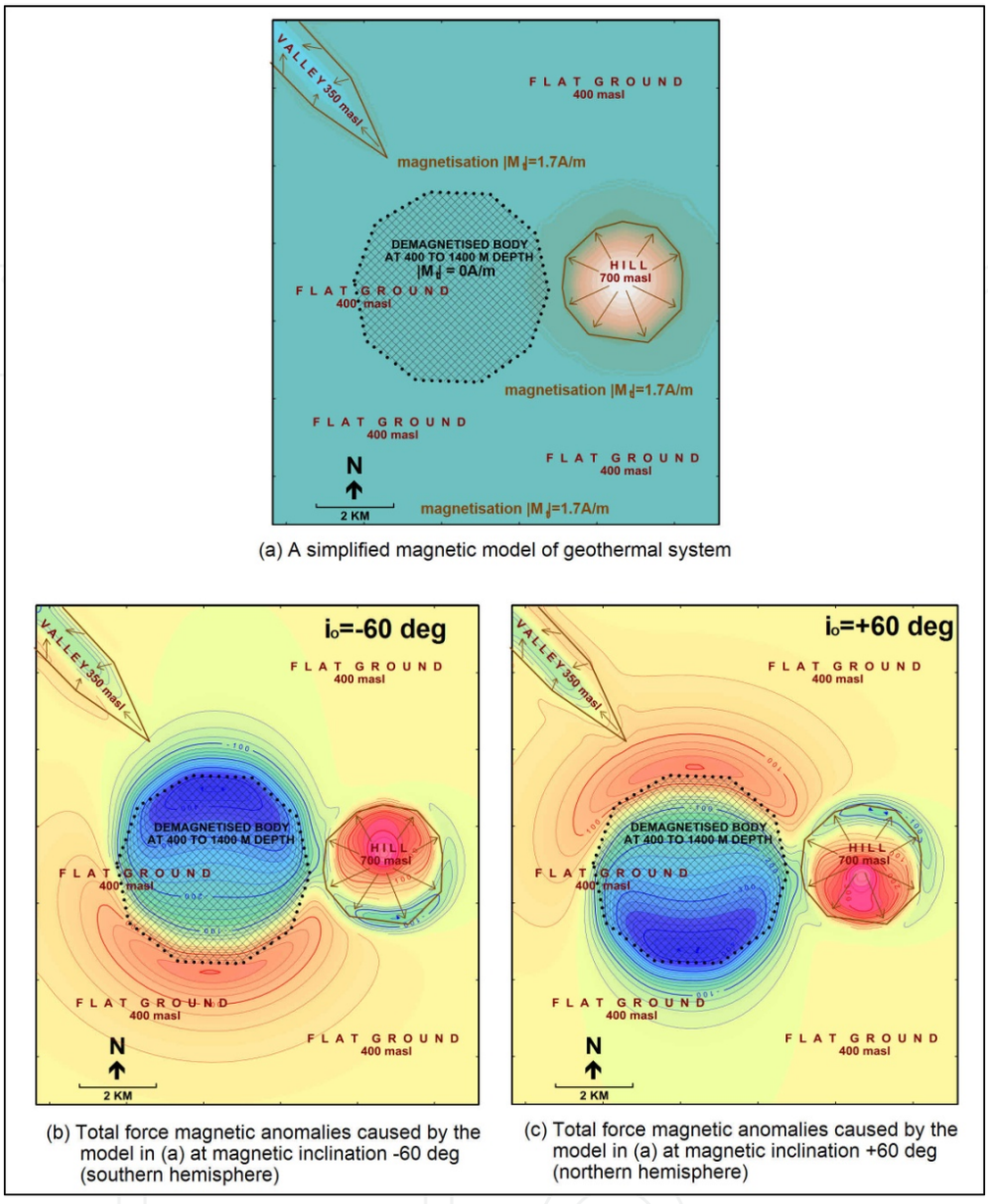

Figure 4. Total force magnetic anomalies (ΔF) caused by a simplified geothermal system at high geomagnetic inclinations of -60° (southern hemisphere) and +60° (northern hemisphere).

4.1.2. In the moderate magnetic inclination

Figure 5 shows the total force anomalies created by the simplified magnetic model at southern hemisphere at geomagnetic inclination of -30° (Figure 5(b) and at northern hemisphere at geomagnetic inclination of +30° (Figure 5(c)). The bipolarity of the total force magnetic anomalies becomes more pronounced and the strengths (magnitudes) of the positive and negative anomalies are roughly equal. The hydrothermally demagnetised rocks can still be identified, but it becomes difficult to delineate their extent directly from the extent of the magnetic anomalies.

http://dx.doi.org/10.5772/61651

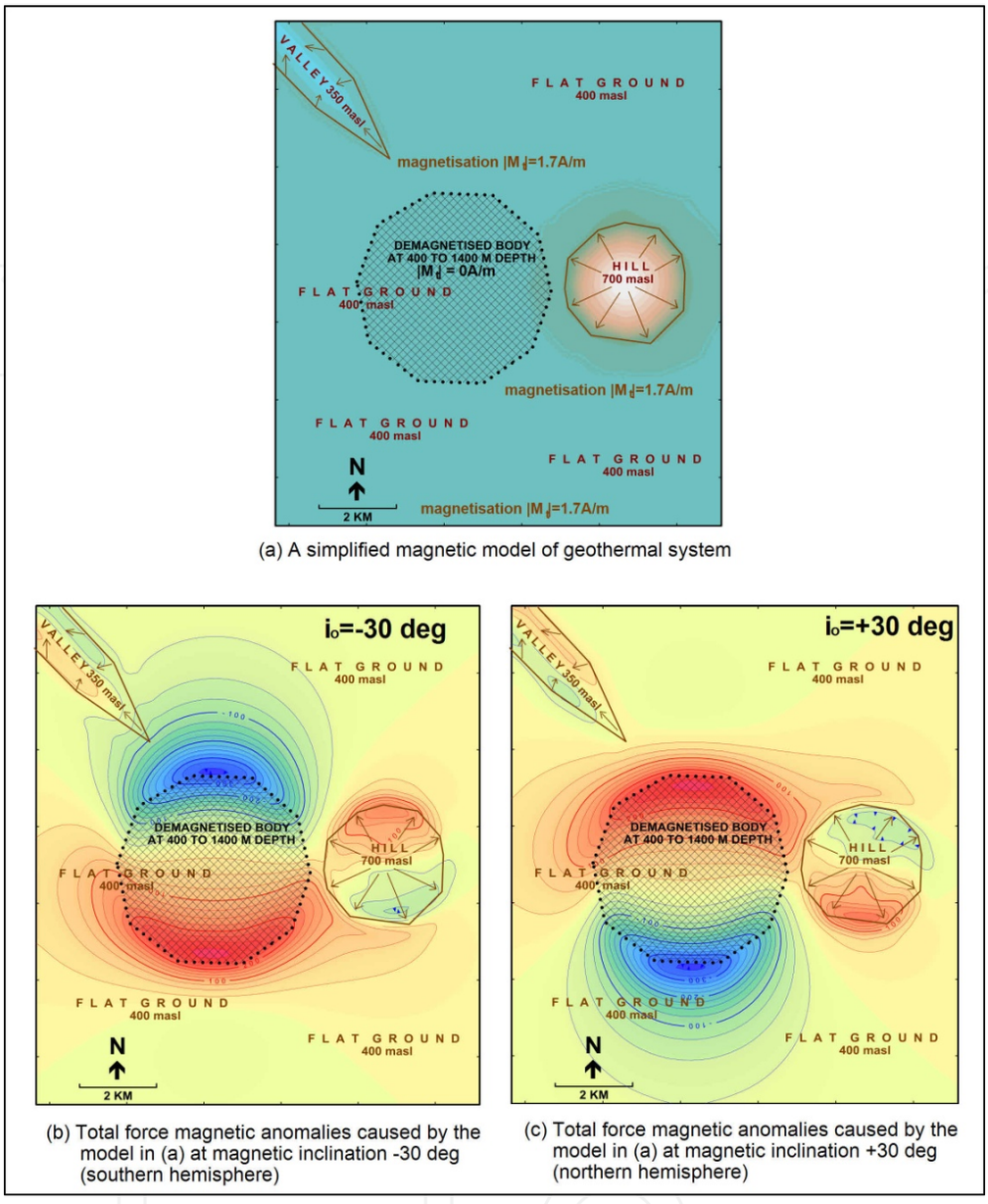

Figure 5. Total force magnetic anomalies (ΔF) caused by a simplified geothermal system at moderate geomagnetic inclinations of -30° (southern hemisphere) and +30° (northern hemisphere).

4.1.3. In the low magnetic inclination

Figure 6 shows the total force anomalies created by the simplified magnetic model at locations close to the magnetic equator, at geomagnetic inclination -10° (Figure 6(b)) and at geomagnetic inclination +10° (Figure 6(c)). Here, the total force magnetic anomalies pattern caused by the geothermal system is much less bipolar but *positive* anomalies become dominant. Hence, it is important to be always aware to this contradictory phenomenon (*negative* magnetisation contrast creating *positive* anomalies). In this low geomagnetic latitude hydrothermally demagnetised rocks are to be identified from positive anomalies, not negative anomalies. The

positive anomalies in Figures 6(a) and 6(b) are clearly recognizable, however the extent of the positive anomaly does not follow the edge of hydrothermally demagnetized rocks very well.

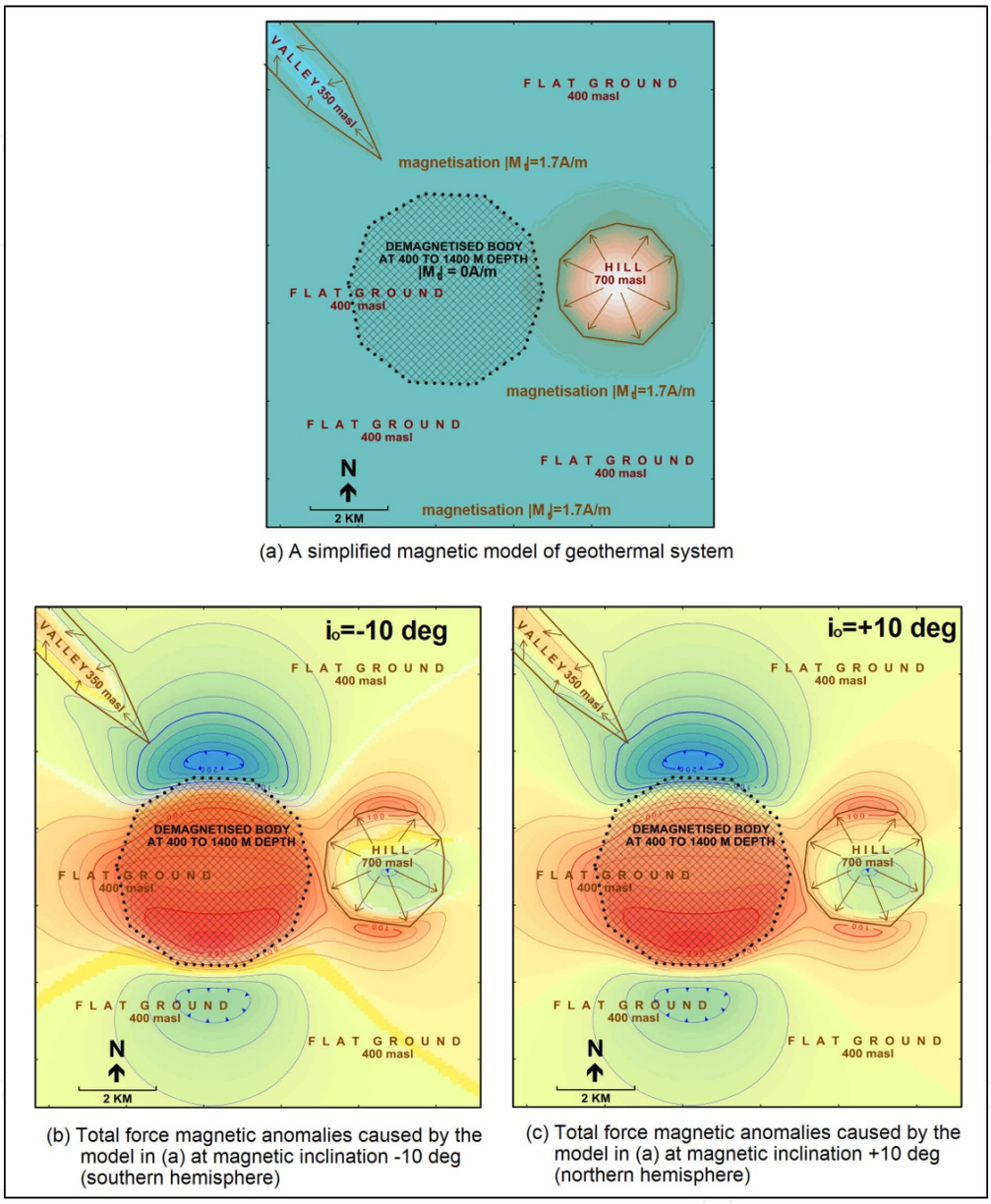

Figure 6. Total force magnetic anomalies (ΔF) caused by a simplified geothermal system at low geomagnetic inclinations of -10° (southern hemisphere close to magnetic equator) and +10° (northern hemisphere close to magnetic equator).

4.1.4. Along the magnetic equator and in the south/north magnetic poles

Figure 7 shows the total force anomalies created by the simple model at two extreme locations, along the magnetic equator where the geomagnetic inclination is 0° (Figure 7(b) and in the south/north geomagnetic pole where the geomagnetic inclination is either -90° or +90° (Figure

http://dx.doi.org/10.5772/61651

7(c)). At the magnetic equator, the hydrothermally demagnetised rocks are marked by dominantly positive anomalies (Figures 7(b)). The positive anomalies are easier to recognise than in Figures 6(b) and 6(c), but their extent still does not accurately follow the extent of the hydrothermally demagnetised rocks. At the magnetic pole (Figure 7(c)) the centre of the hydrothermally demagnetised rocks is marked by the centre of strong magnetic low (negative anomalies). Here, it is also easy to trace or delineate the edges of the hydrothermally demagnetised rocks (the geothermal reservoir) from the edges of the magnetic low. Hence, the location of geothermal reservoir would be able to be delineated directly if the reservoir is located in the south/north magnetic pole.

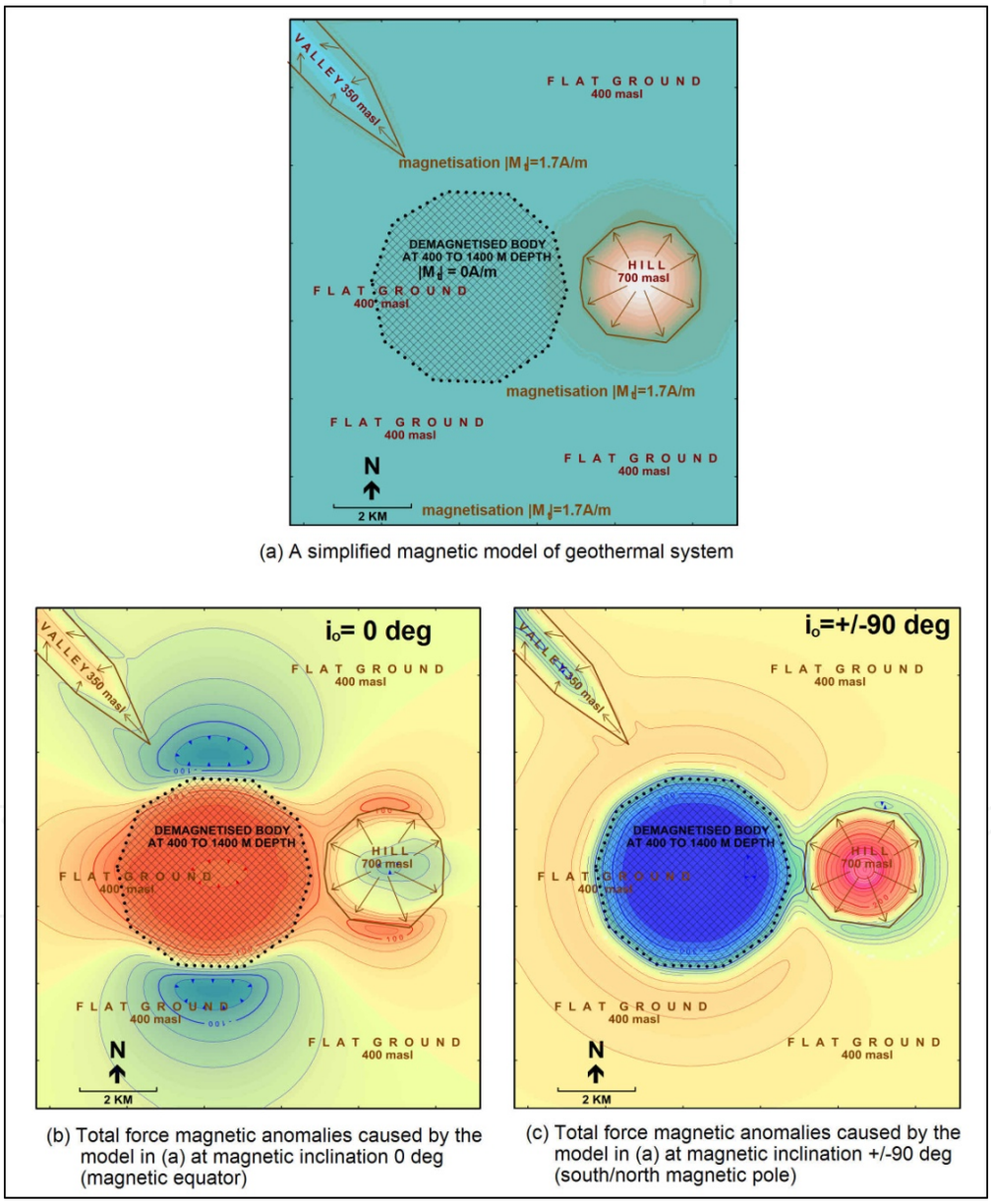

Figure 7. Total force magnetic anomalies (ΔF) caused by a simplified geothermal system geomagnetic inclinations of 0° (along the magnetic equator) and +/-60° (the magnetic south/north pole).

4.2. Delineating the likely extent of geothermal reservoir from total force magnetic anomalies

The previous section (Section 4.1) has shown that total force magnetic anomalies associated with a geothermal system have different patterns at different geomagnetic inclinations (geographical locations). At high magnetic inclinations (±60°to ±90°) a demagnetised geothermal reservoir is marked by negative total force magnetic anomalies. At the magnetic south and north poles (magnetic inclinations of -90° and +90°) the edges of the (theoretical) geothermal reservoir can be delineated directly from the edges of the magnetic low, even when the background volcanic rocks hosting the geothermal reservoir are not magnetically homogeneous. As the location moves away from the magnetic pole(s), it becomes less easy to delineate the geothermal reservoir. At geomagnetic inclinations of around +/- 30°, it becomes impossible to delineate the geothermal reservoir from the extents of the total force magnetic anomalies. However, it is possible to transform the total force magnetic anomalies into the situation that would be observed if the causative source is located in the magnetic pole, using a standard magnetic operation known as "reduction to pole" (RTP). This operation was first introduced by Baranov [1]. The operation moves centres of anomaly to positions above their sources [3], assuming that the rock total rock magnetisation $(\mathbf{m}_t)$ is either parallel of directly opposes the direction of $\mathbf{B}_o$, which is true for the case of young Quaternary volcanic rocks. However, as the magnetic latitude approaches its equator, the RTP operator becomes unbounded along the direction of magnetic declination and therefore amplifies the noise in this direction to the extent that the resultant RTP field is dominated by linear features aligned with the direction of declination [18]. The solution to this problem has now become available by using specially designed variations of the RTP transform. User friendly software packages that can perform the RTP operation and address the problem of low magnetic inclination are now available online.

Figures 8, 9 show the results of RTP operation using the Oasis Montaj software applied to our theoretical total force anomalies shown in Figures 4, 5 6 and 7.

In Figures 8, the total force magnetic anomalies at geomagnetic inclinations +/-60° and +/-30° that have been reduced to pole (RTP) can accurately trace the extent of the hydrothermally demagnetised rocks. The hydrothermally demagnetised rocks can also be traced from the total force magnetic anomalies close to the magnetic equator shown in Figure 9, but the tracing (delineation) of their edges becomes slightly more difficult. The opposite transformation of reduction to magnetic equator (RTE) (available in the Oasis Montaj software package) would not help much in solving the problem, as the total force magnetic high at the equator does not accurately follow the edge if the hydrothermally demagnetised rocks either (Figure 7 (b)). In general, the closer the location is to the magnetic equator, the more difficult it is to delineate the source body from the total force magnetic anomalies. A quantitative 3D modelling will help, but conducting this complex and difficult task would be required only if detailed delineation of hydrothermally demagnetised rocks is crucial and absolutely necessary.

http://dx.doi.org/10.5772/61651

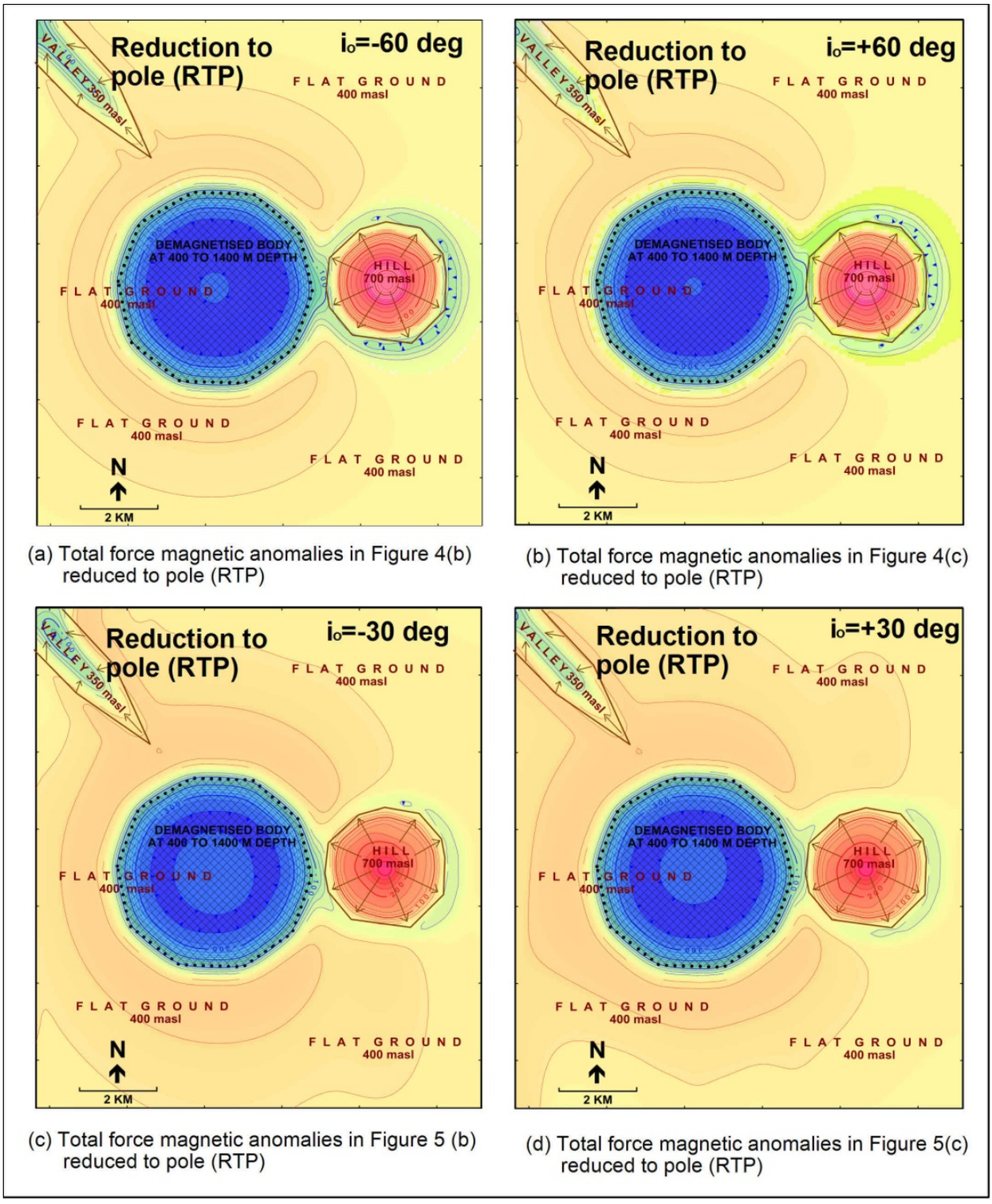

(a) Total force magnetic anomalies in Figure 4(b) reduced to pole (RTP)

(b) Total force magnetic anomalies in Figure 4(c) reduced to pole (RTP)

(c) Total force magnetic anomalies in Figure 5 (b) reduced to pole (RTP)

(d) Total force magnetic anomalies in Figure 5(c) reduced to pole (RTP)

Figure 8. Reduction to pole (RTP) of total force magnetic anomalies (ΔF) caused by a simplified geothermal system at geomagnetic inclinations of +/-60˚ and +/-30˚.

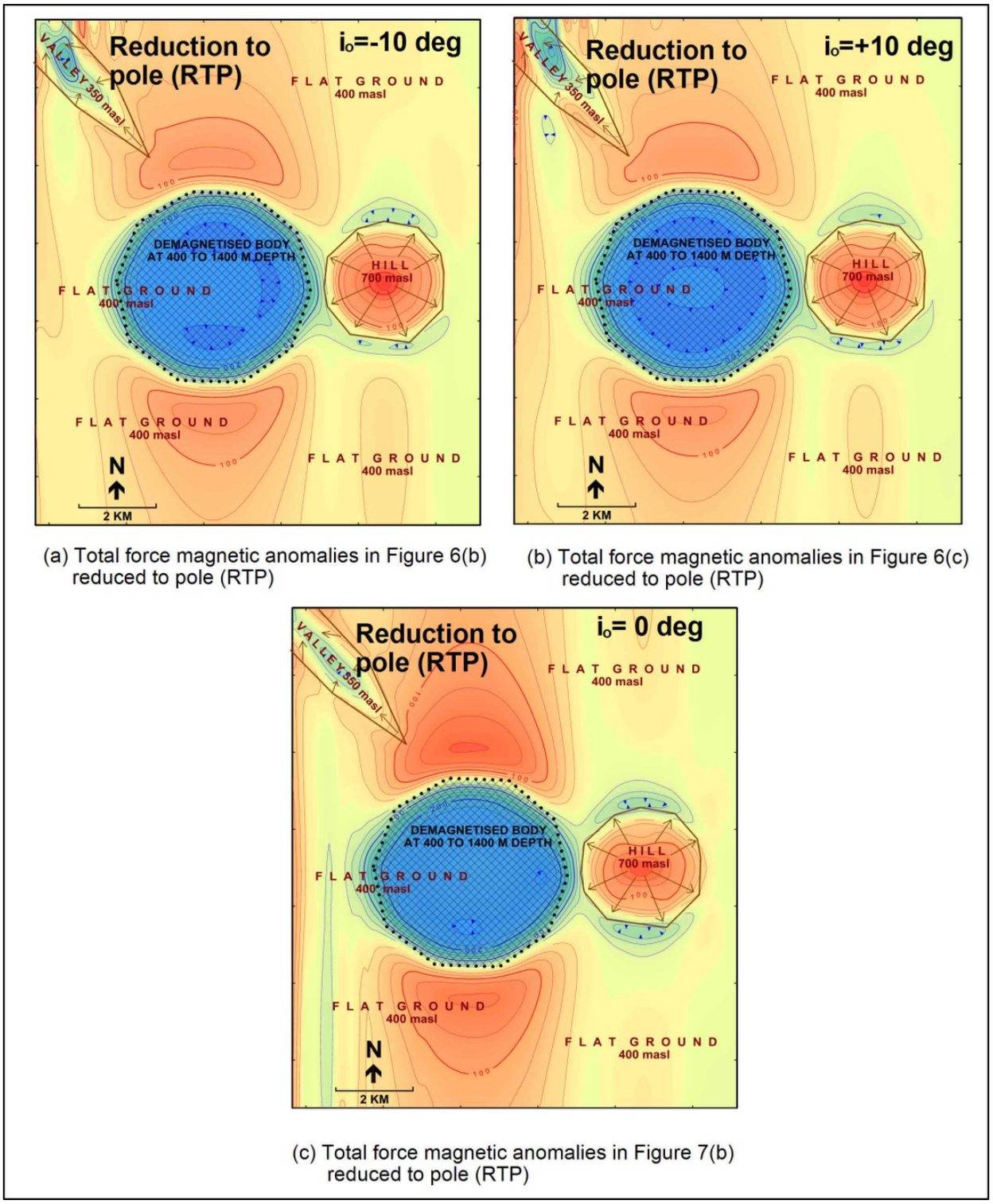

Figure 9. Reduction to pole (RTP) of total force magnetic anomalies (ΔF) caused by a simplified geothermal system at geomagnetic inclinations of +/-10° (close to the magnetic equator) and 0° (along the magnetic equator).

http://dx.doi.org/10.5772/61651

5. Examples of airborne magnetic surveys to investigate high temperature geothermal reservoirs

5.1. Introduction

A new, simple but effective, interpretation approach of airborne magnetic survey for investigation of high temperature geothermal resources in Quaternary volcanic setting has been introduced and discussed in the previous sections. To gain a more comprehension of its practical aspects, the interpretation approach is applied to real airborne magnetic data from the TVZ in New Zealand (geomagnetic inclination about -65˚) and from the eastern Java Island in Indonesia (geomagnetic inclination about -35˚). These examples of interpretations are presented and discussed in the following sections. Note that all the magnetic interpretations presented are new interpretations, specifically carried out to illustrate the approach introduced previously in this chapter. The gridding, plotting contouring and drawing, trend determinations and RTP transformations of the anomalies are all carried out using the Oasis Montaj software package.

5.2. Examples from TVZ, New Zealand

5.2.1. Wairakei geothermal field

The high temperature Wairakei geothermal field in the TVZ is the first geothermal field used for electricity generation in New Zealand, and the second in the world after the Larderello geothermal field in Italy. The geothermal system is situated in rather flat topography (Figure 10). The geothermal reservoir was delineated using Schlumberger DC resistivity surveys and the boundary shown in Figure 10 has been slightly refined using information from a few geothermal boreholes. To the southeast of Wairakei is another high temperature field, the Tauhara geothermal field. Both Wairakei and Tauhara reservoir are hosted by Quaternary volcanic rocks. The fields are located at a high magnetic inclination of about -65˚. Figure 11 shows the map of $|\mathbf{B}_{obs}|$ over the Wairakei field and the northern part of the Tauhara field obtained from a detailed airborne magnetic survey draped 60 m above ground which was conducted by the gold exploration company Glass Earth NZ Ltd in 2006, and from a previous smaller survey at similar altitude conducted by the GNS Science in 1989. The 1st order trend of $|\mathbf{B}_{obs}|$ to estimate $|\mathbf{B}_o|$ is also shown in Figure 11. Figure 12 presents the total force magnetic anomalies (ΔF) map over the area.

The total force magnetic anomalies after the reduction to pole (RTP) transformation are shown in Figure 13. The magnetic anomalies (RTP) shown in this figure are located directly above their causative sources. Prominent magnetic lows are present in the north-western part of the Wairakei field and over the Tauhara field. These magnetic lows represent intensive and/or thick hydrothermal demagnetisation. Less prominent magnetic low can be seen over the fumaroles and steaming ground at Crater of the Moon, representing hydrothermal demagnetisation by acidic condensate in the shallow vapour zones. The prominent magnetic low in the north-western part of the Wairakei field suggests that in this area the Wairakei geothermal

reservoir extends beyond the field boundary defined by resistivity survey, although the possibility that part of the negative anomalies outside the boundary of the geothermal field are due to by reversely magnetised rocks cannot be completely ruled out.

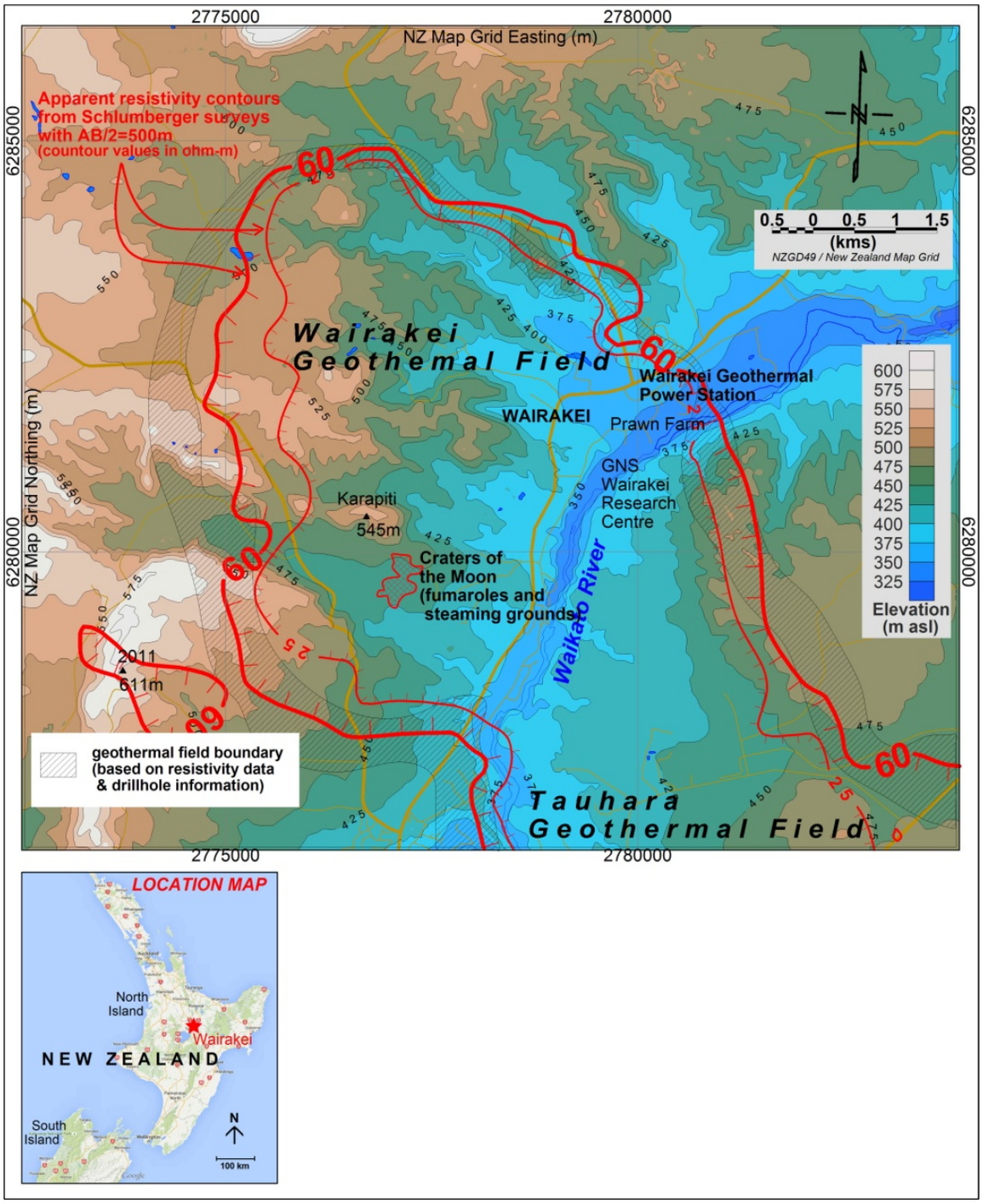

Figure 10. Topographic map of the Wairakei and the northern part of Tauhara geothermal fields in the TVZ (New Zealand) showing the boundary of the fields based on Schlumberger DC resistivity survey.

http://dx.doi.org/10.5772/61651

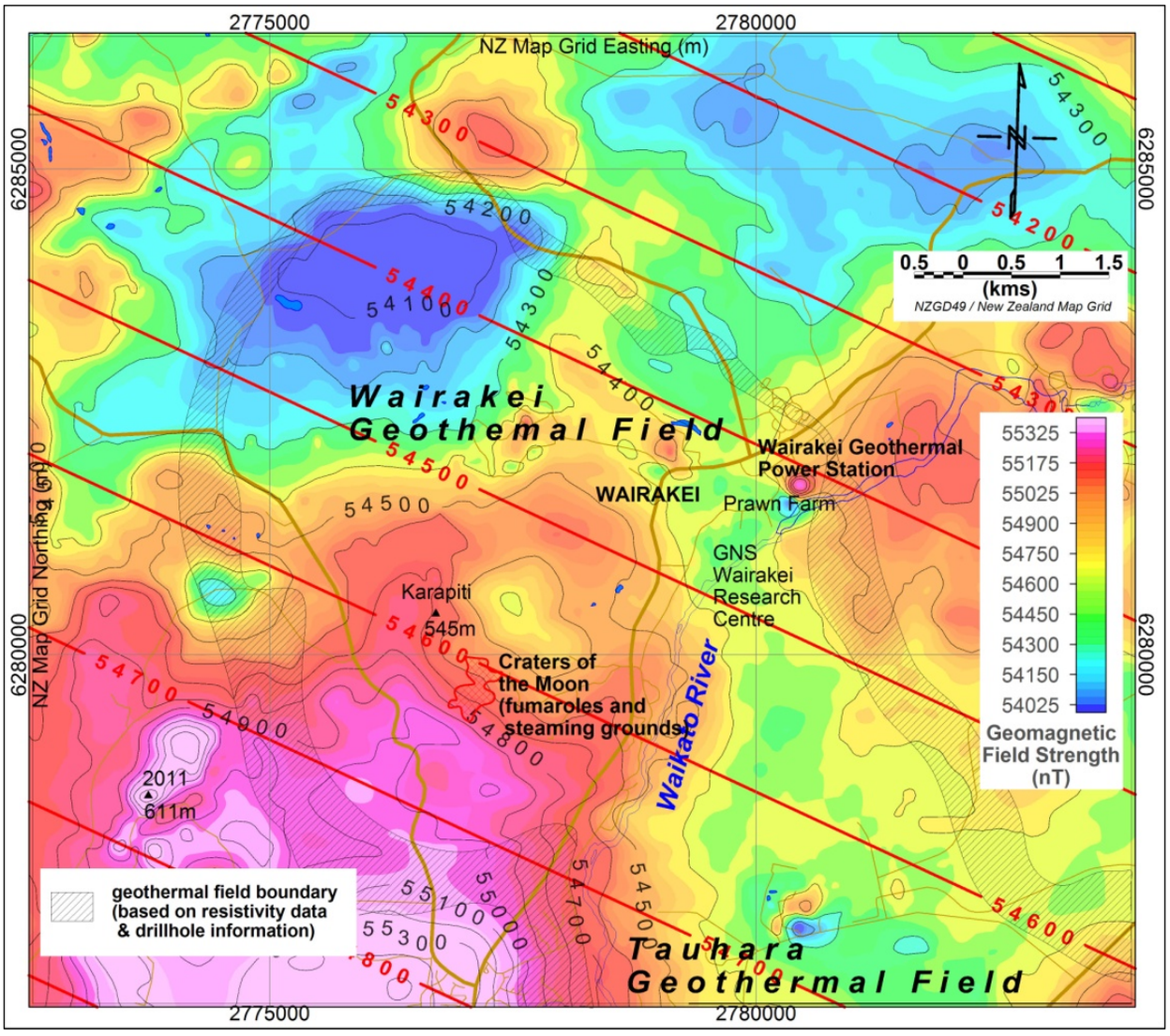

Figure 11. Map of observed total force geomagnetic field strengths ($|\mathbf{B}_o|$) over the Wairakei and the northern part of Tauhara geothermal fields in the TVZ (New Zealand). The red contour lines represent $|\mathbf{B}_o|$ values as defined by the first order trend of all $|\mathbf{B}_{obs}|$ across the area.

5.2.2. Mokai geothermal field

The high temperature Mokai geothermal field is also located in the Taupo Volcanic Zone, about 20 km west of the Wairakei field. The Mokai geothermal reservoir is also hosted by Quaternary volcanic rocks and has slightly steeper topography than the Wairakei field (Figure 14).

Figure 14 shows the boundary of Mokai geothermal field delineated from Schlumberger DC resistivity surveys, and the surface thermal manifestations of the field. The 60 ohm-m resistivity contour is extending northeast-north toward the thermal springs in a lower elevation, indicating lateral outflow of geothermal water. Figure 15 shows the map of $|\mathbf{B}_{obs}|$ over the Mokai geothermal field obtained from the same detailed survey by Glass Earth Ltd. in 2006

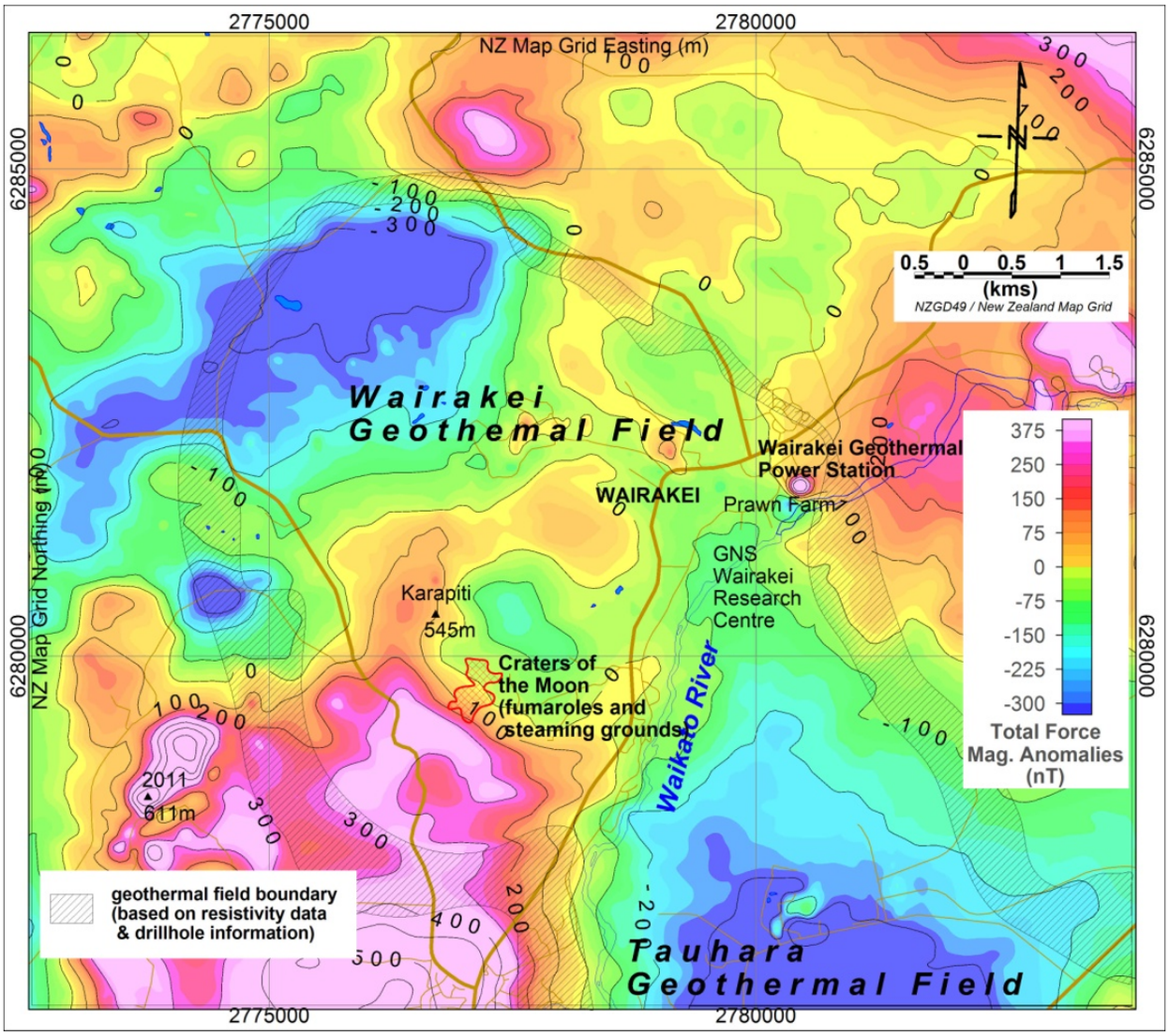

Figure 12. Map of total force magnetic anomalies (ΔF) over the Wairakei and the northern part of Tauhara geothermal fields in the TVZ (New Zealand). The ΔF values were obtained by subtraction of $|\mathbf{B}_o|$ determined from 1st order trend of $|\mathbf{B}_{obs}|$.

that covers the Wairakei field. The 1st order trend of $|\mathbf{B}_{obs}|$ to estimate $|\mathbf{B}_o|$ is also shown in the map. The total force magnetic anomalies (ΔF) map the Mokai area is shown in Figure 16. A broad magnetic low appears associated with the geothermal field at location slightly shifted to the north. Several other magnetic lows are present outside the Mokai geothermal field to the northwest, southwest, southeast and further to the northeast of the Mokai resistivity boundary.

Reduction to pole (RTP) transformation was applied to the total force anomalies in Figure 16 and the result is presented in Figure 17. In this figure, the magnetic low above the Mokai geothermal field becomes consistent with the resistivity boundary, indicating that hydrother-

http://dx.doi.org/10.5772/61651

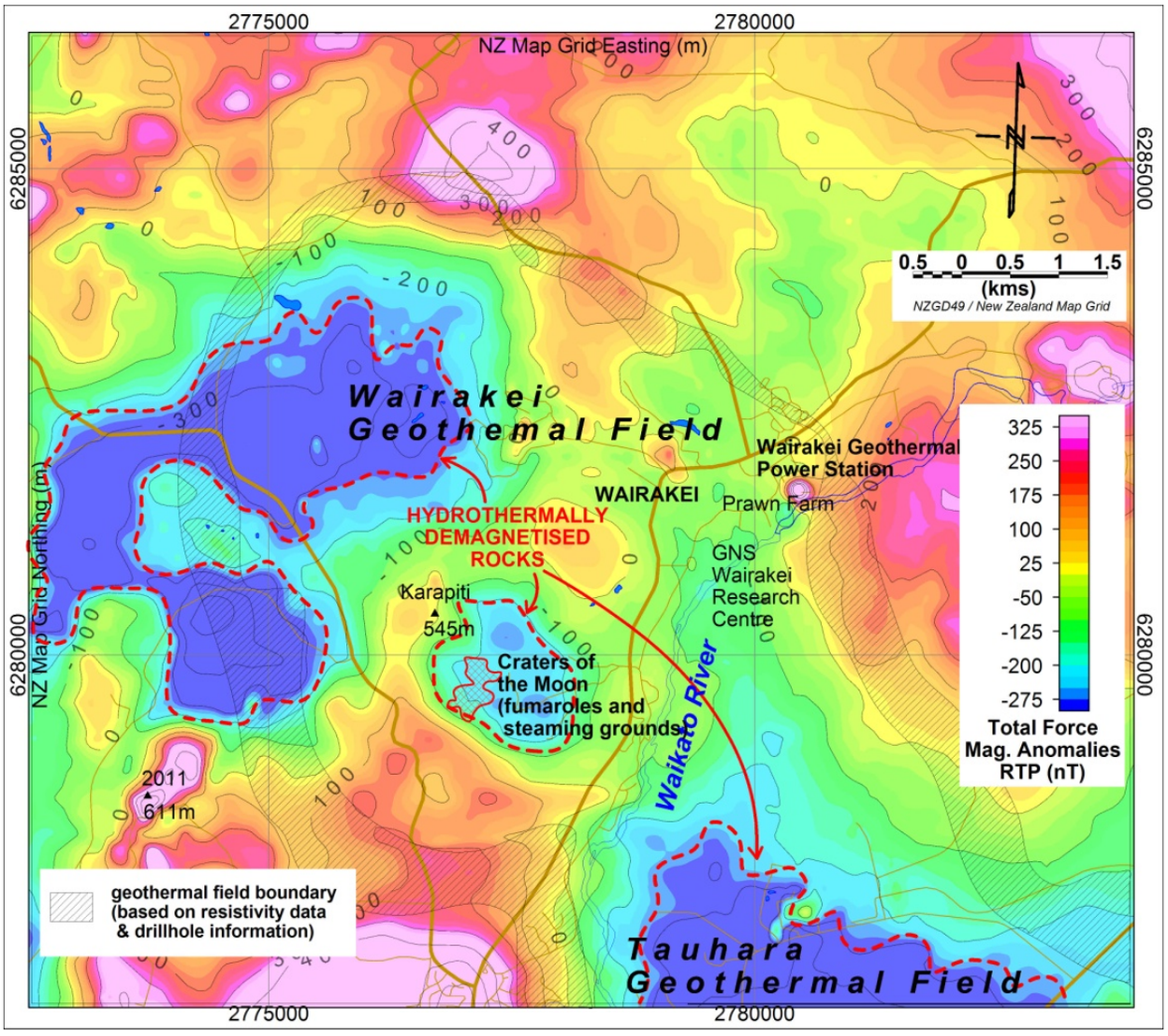

Figure 13. The result of reduction to pole (RTP) of the total force magnetic anomalies (ΔF) over the Wairakei and the northern part of Tauhara geothermal fields in the TVZ (New Zealand).

mally demagnetised rocks are present in the Mokai Reservoir. Moderately low magnetic RTP anomalies mark the western part of Pukemoremoe rhyolite topographic dome, suggesting that acidic condensate formed in shallow vapour zones here has caused hydrothermal demagnetisation. Reversely magnetised rocks are known to be present in this area [28]. Hence, the magnetic lows outside the Mokai geothermal field boundary could represent reversely magnetised rocks, as indicated in Figure 16. The magnetic low caused by the hydrothermally demagnetised rocks inside the Mokai reservoir shows variation in strength. This variation could be caused the variation of intensity and/or thickness of the hydrothermal demagnetisation process, which could held clue to the variation of reservoir permeability and/or movement of geothermal water. This could be investigated further by a quantitative 3D modelling of the magnetic anomalies.

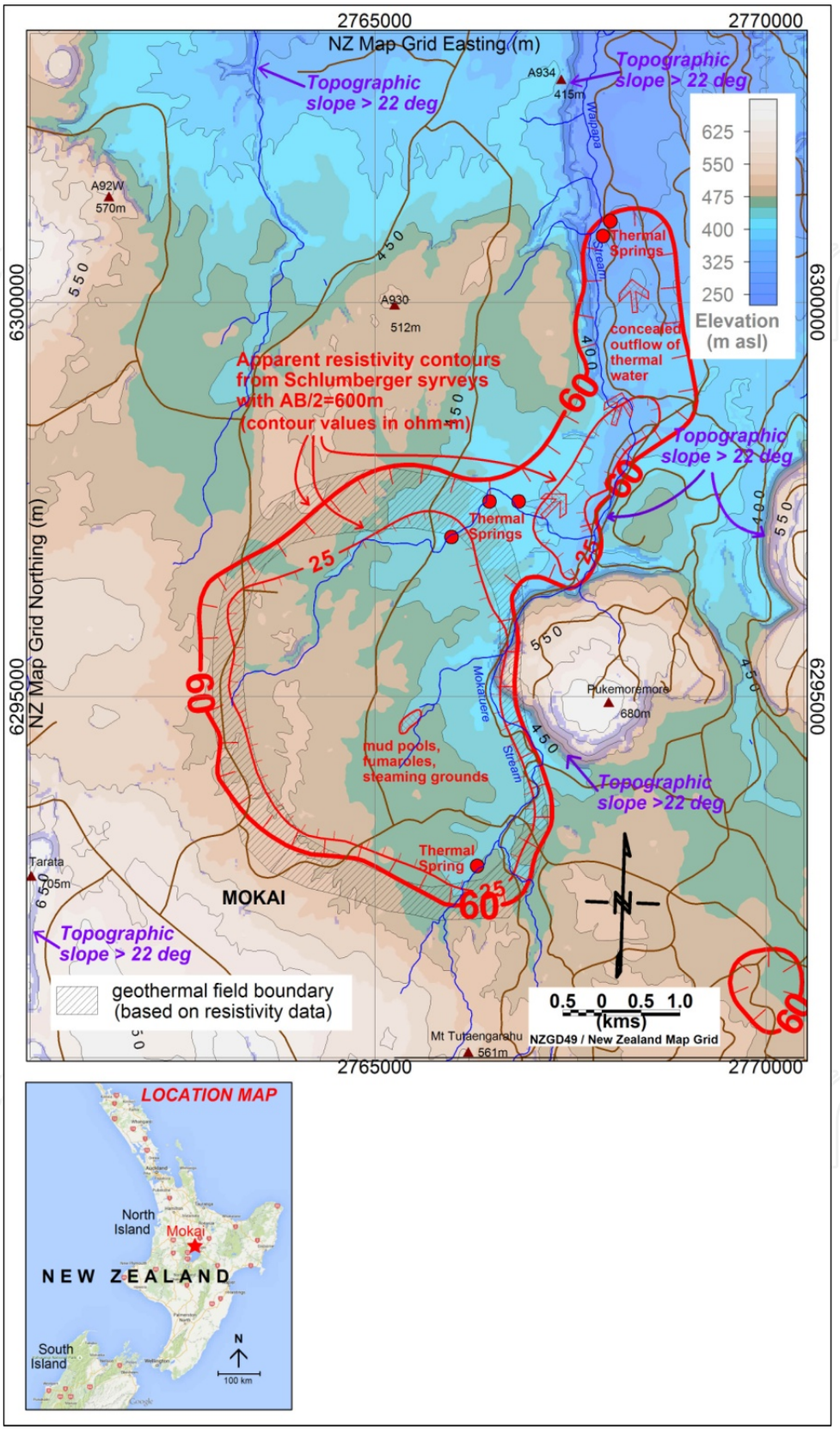

Figure 14. Topographic map of the Mokai geothermal field in the TVZ (New Zealand) showing the boundary of the field based on Schlumberger DC resistivity survey.

http://dx.doi.org/10.5772/61651

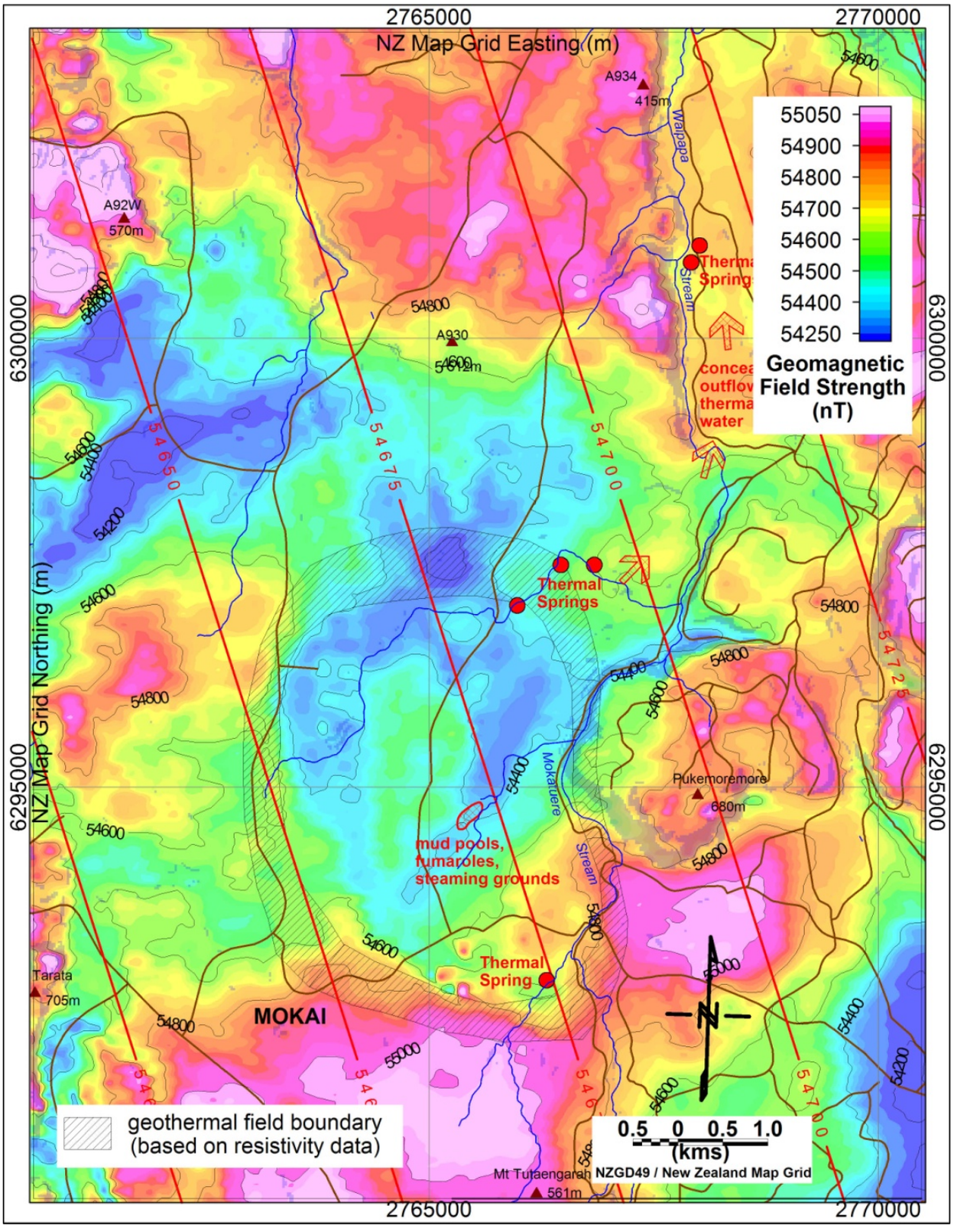

Figure 15. Map of observed total force geomagnetic field strengths ($|\mathbf{B}_o|$) over the Mokai geothermal field in the TVZ (New Zealand). The red contour lines represent $|\mathbf{B}_o|$ values as defined by the first order trend of all $|\mathbf{B}_{obs}|$ across the area.

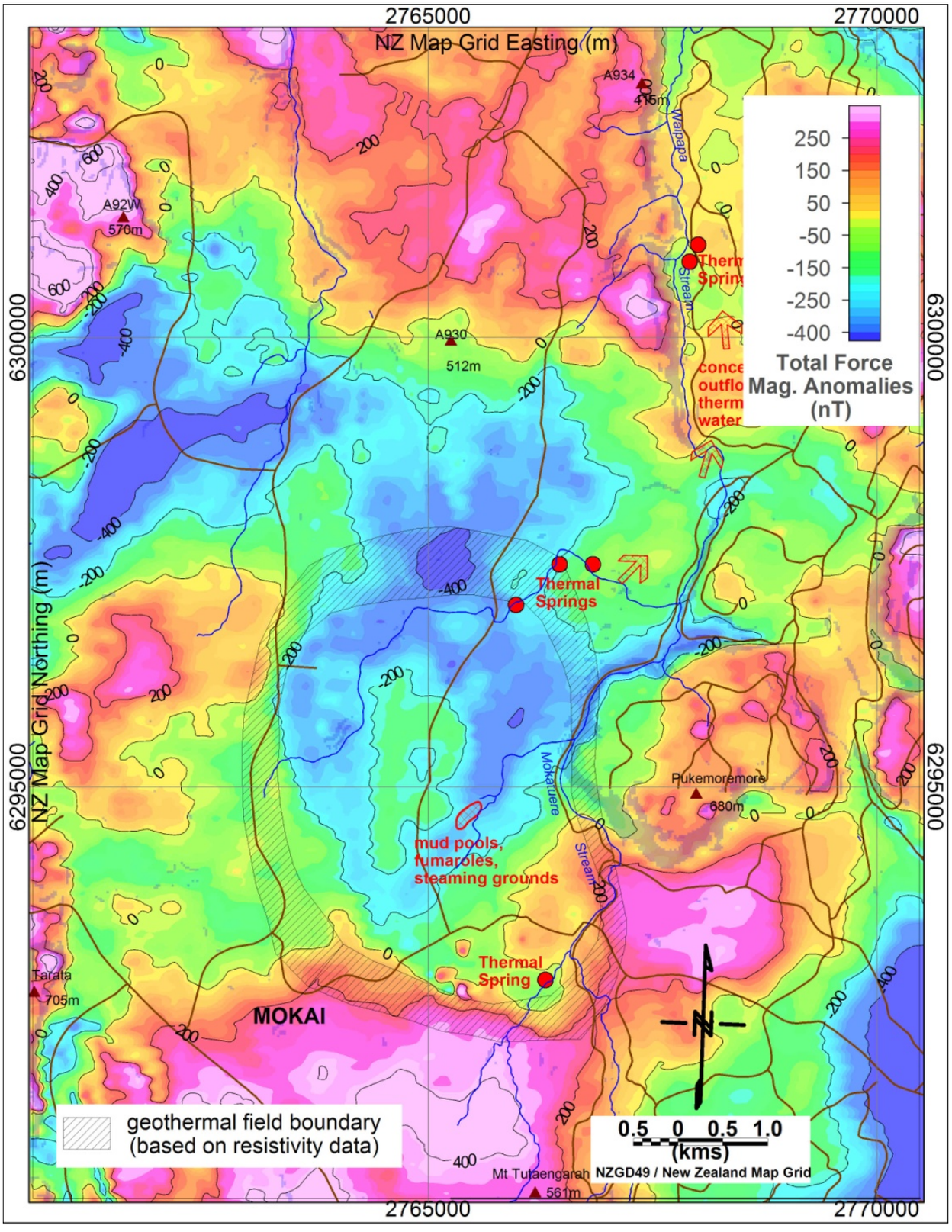

Figure 16. Map of total force magnetic anomalies (ΔF) over the Mokai geothermal field in the TVZ (New Zealand). The ΔF values were obtained by subtraction of $|\mathbf{B}_o|$ determined from 1st order trend of $|\mathbf{B}_{obs}|$.

http://dx.doi.org/10.5772/61651

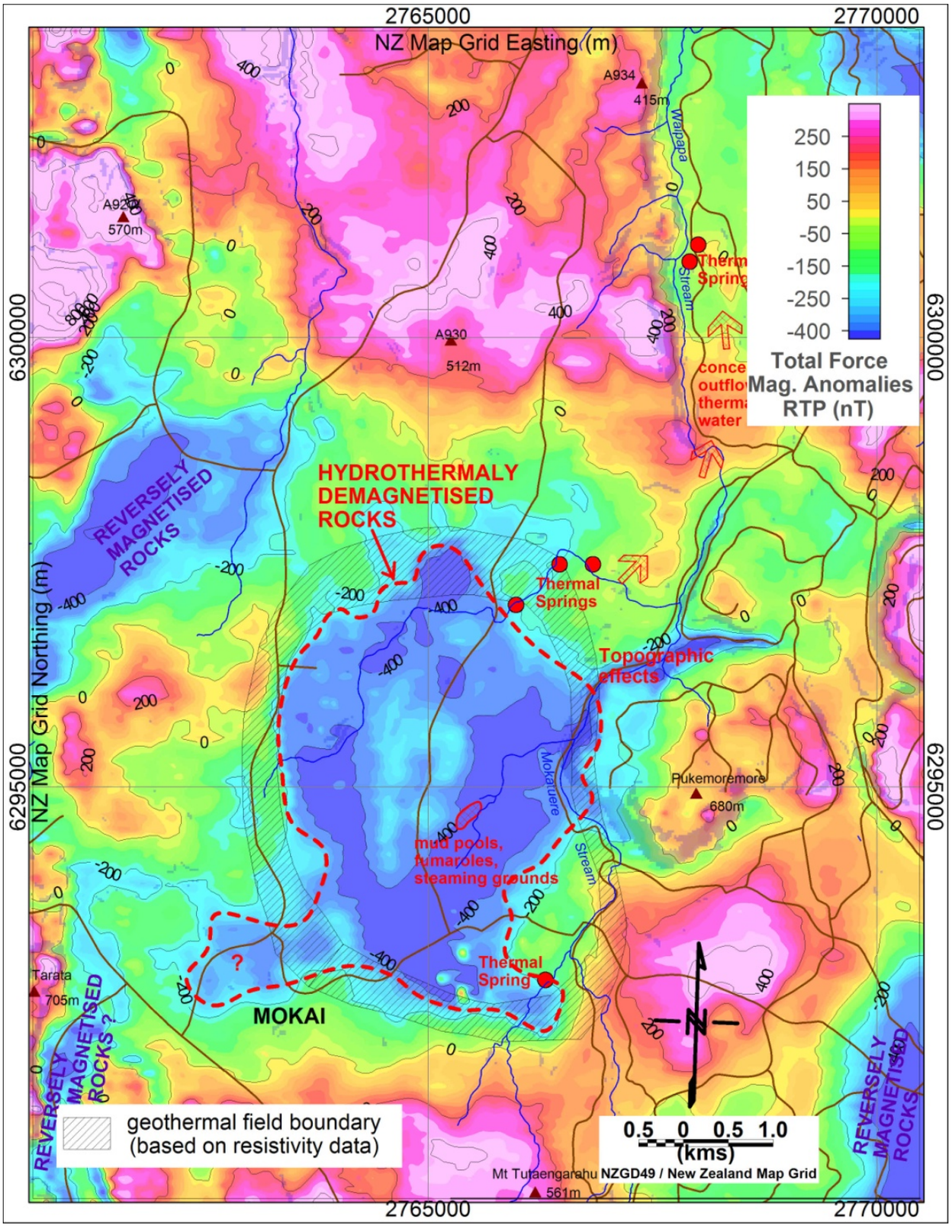

Figure 17. The result of reduction to pole (RTP) of the total force magnetic anomalies (ΔF) over the Mokai geothermal field in the TVZ (New Zealand).

5.3. Example from Java Island, Indonesia

5.3.1. Ijen geothermal field

The Ijen geothermal field is located in eastern Java Island of Indonesia (see the location map in Figure 18) with a geomagnetic inclination of about -35°. The airborne magnetic survey over the Ijen geothermal field was carried out in 1990 by Penas-Carson Services Inc. (USA) for the Indonesia Pertamina Geothermal Division. The survey was made at flight elevation of about 1 km above the ground, along west-east flight lines separated by about 0.75-1 km spacing. The Ijen geothermal field is hosted by Quaternary andesitic volcanic rocks which form steep topography around the field. Figure 18 shows the topography of the Ijen area and the locations of surface thermal manifestation of the geothermal field consisting of altered rocks near Telagawaru and a group of thermal springs near Blawan in the north. The "raw" airborne magnetic data were presented by the Penas-Carson Inc., which were obtained by reducing the IGRF variation from the measured geomagnetic field. Such "raw" airborne magnetic data are shown in Figure 19, together with their 1st order trend. Figure 20 shows the total force magnetic anomalies (ΔF) over the Ijen area. In this figure the bipolar anomalies associated with Mt Suket, Mt Pendil and Mt Rante become clearly visible. Less clearly shown is the bipolar anomaly over Mt Ijen. Positive anomalies are also seen over the north-eastern Kendeng Ridge. A wide magnetic low is presents over the geothermal field region. The north-eastern part of this magnetic low could be the negative part of the bipolar magnetic anomaly of the north east Kendeng Ridge. Because of the moderate magnetic inclination of the region, the ΔF values shown in Figure 20 are likely to spread widely over the causative sources. A direct interpretation of this figure can be misleading without the RTP transformation.

The total force anomalies over the Ijen geothermal area after reduction to pole (RTP) transformation are shown in Figure 21. The magnetic anomalies (RTP) shown in this figure would be located above their causative sources. The most interesting magnetic RTP anomalies in Figure 21 is the magnetic low that appears to be associated with the outcrop of altered rocks west of Telagawaru. This magnetic low is interpreted in Figure 21 to represent hydrothermally demagnetised rocks. This leads to the inferred model of Ijen geothermal system consisting of a geothermal up-low zone in the Telagawaru – Mt Genteng area and concealed outflow of thermal water towards the thermal springs near Blawan. The magnetic low to the northwest of Kendeng Ridge could represent reversely magnetised Quaternary volcanic rocks. Reversely magnetised rocks are probably also the sources of the three magnetic lows near the southern edge of Figure 21. Positive anomalies marked Mt Suket, Mt Pendil, Mt Rante and Mt Ijen, showing that these mountains are formed by normally magnetised rocks. The magnetic high which follows the north-eastern Kendeng Ridge in Figure 20 has moved in Figure 21 to a new location to be entirely southwest of the ridge. This magnetic high probably represents a subsurface lava body underneath.

http://dx.doi.org/10.5772/61651

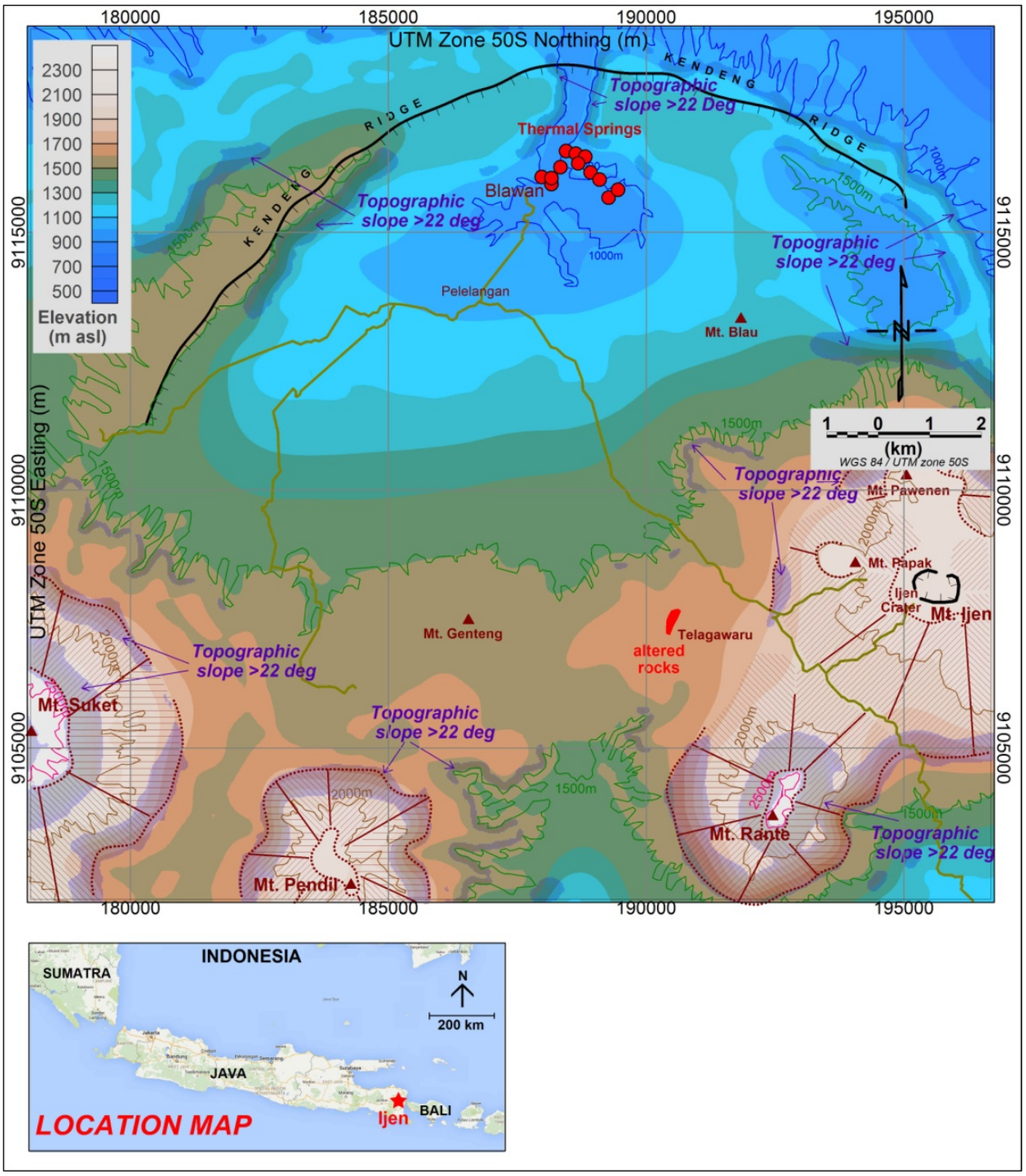

Figure 18. Topographic map of the Ijen geothermal field in the Eastern Java (Indonesia) showing the prominent topography of the surrounding Mt. Suket, Mt. Pendil, Mt Rante and Mt Ijen and the surface thermal manifestations (altered rocks and thermal springs) of the field.

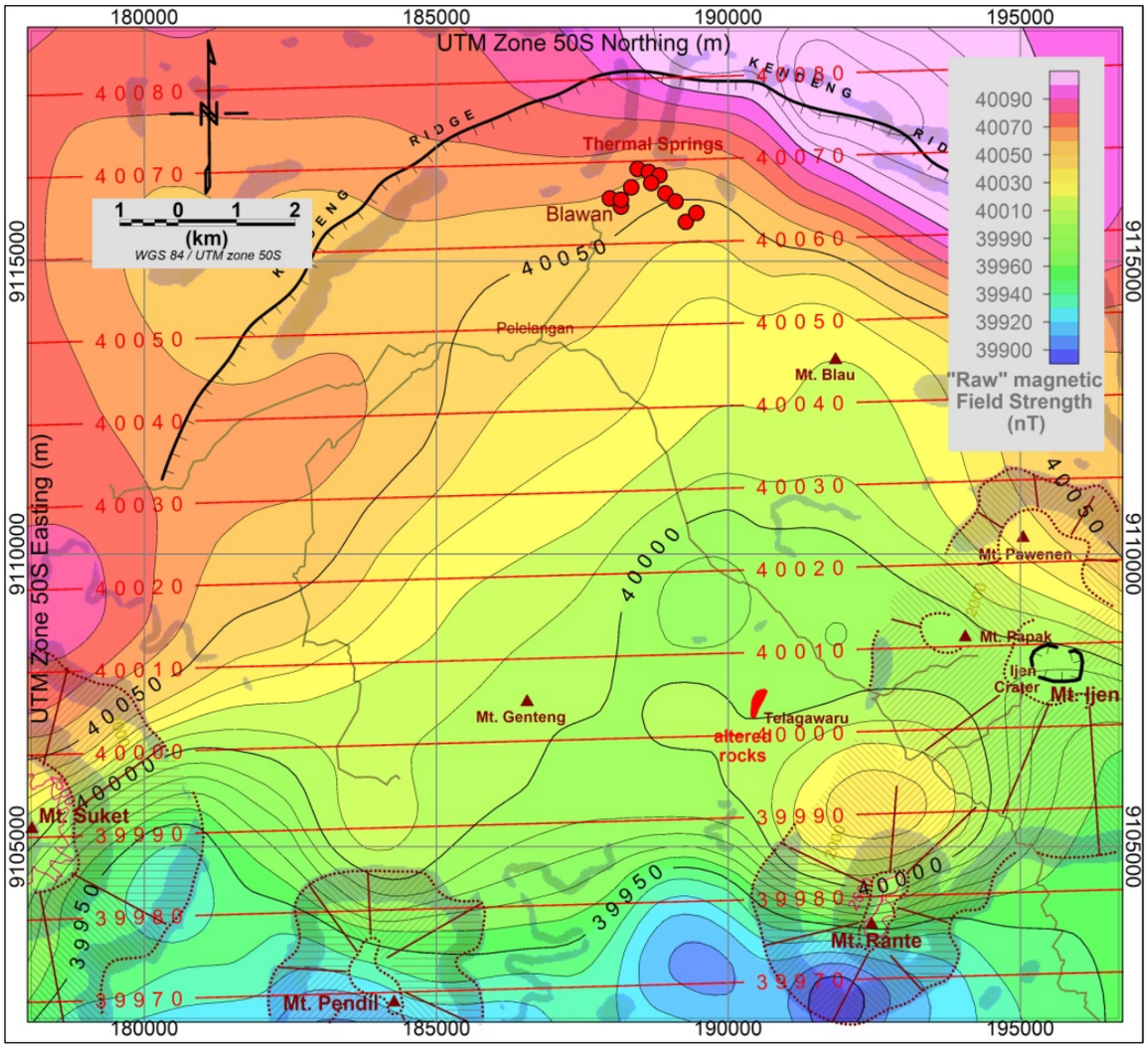

Figure 19. Map of observed total force "raw" field strengths ($\sim|\mathbf{B}_{obs}|$) over the Ijen geothermal field in the eastern Java (Indonesia). The red contour lines represent $|\mathbf{B}_o|$ values as defined by the first order trend of all $\sim|\mathbf{B}_{obs}|$ across the area.

6. Summary and discussion

This chapter has shown that airborne magnetic data can be very useful in the investigation of high temperature geothermal reservoirs hosted by Quaternary volcanic rocks, particularly in the area with difficult ground access. Data might be already available over the geothermal target area from some previous surveys by mineral exploration companies or government institutions. To carry out a new airborne magnetic survey, many geophysical exploration companies are advertising their service and can be contacted on the internet, some of them can do the survey almost anywhere in the world. Even when a new survey is required, the airborne magnetic survey should still be a cost-effective method to explore and investigate high temperature geothermal resources in Quaternary volcanic setting.

http://dx.doi.org/10.5772/61651

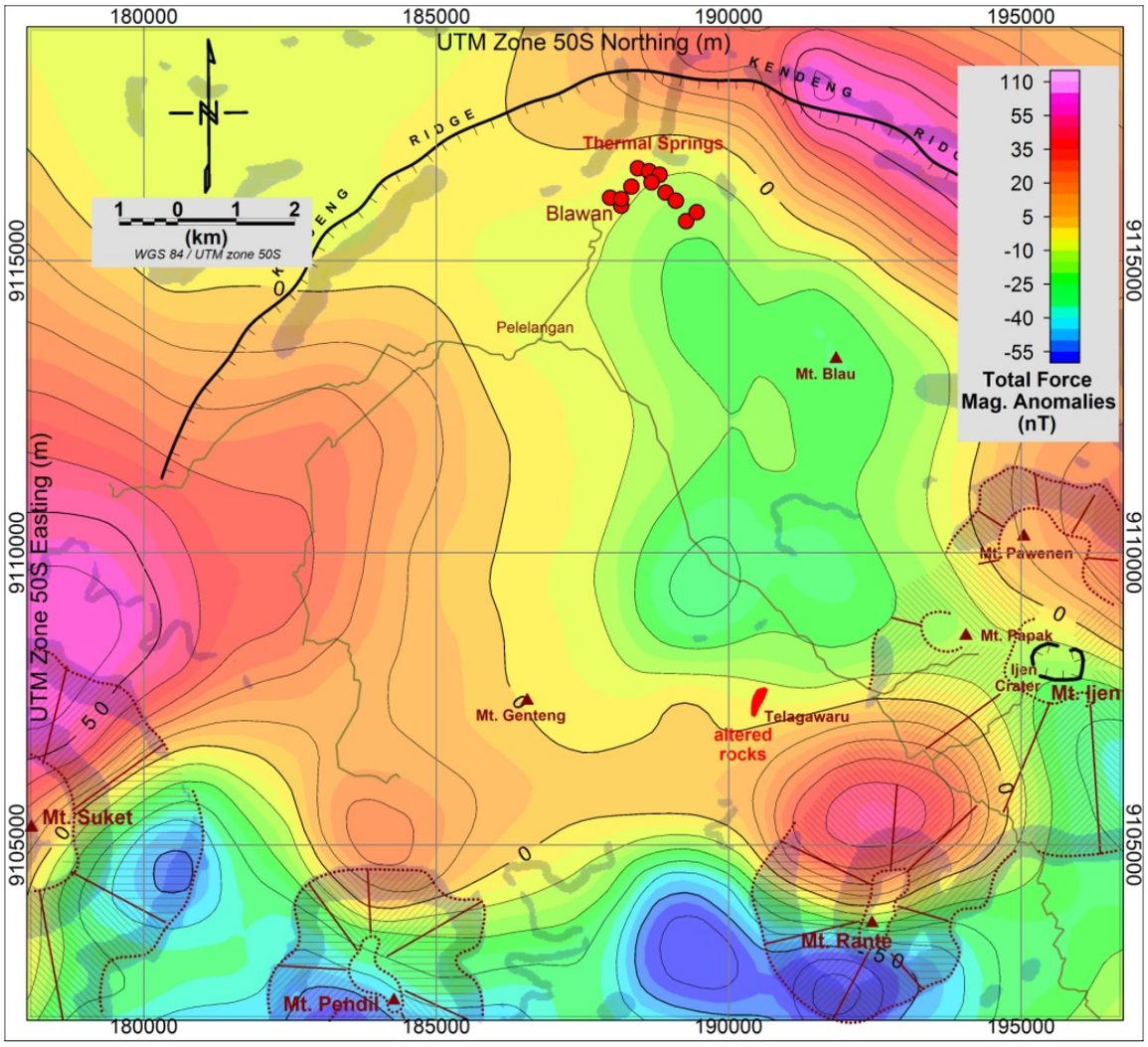

Figure 20. Map of total force magnetic anomalies (ΔF) over the Ijen geothermal field in the eastern Java (Indonesia). The ΔF values were obtained by subtraction of $|\mathbf{B}_o|$ determined from 1st order trend of ~$|\mathbf{B}_{obs}|$.

Various aspects of the application of airborne magnetic survey for the geothermal investigation are presented and explained in this chapter. The total force magnetic anomalies (ΔF) which are the first result obtained from an airborne magnetic survey are explained in considerable details, including how to approximately obtain ΔF values that reflect only the variation of magnetisation no deeper than the "survey target". Simple but effective diagrams to predict total force magnetic anomalies due to a magnetic dipole at different geomagnetic latitudes are introduced. These diagrams provide a basic knowledge for the application of airborne magnetic survey to investigate a variety of geological features, including high temperature geothermal reservoirs. A demagnetised geothermal reservoir has a negative magnetisation contrast. At high magnetic latitudes (away from the magnetic equator) a demagnetised reservoir is marked by dominantly negative total force magnetic anomalies. However, near the magnetic equator, the opposite occurs that the demagnetised reservoir is marked by dominantly positive

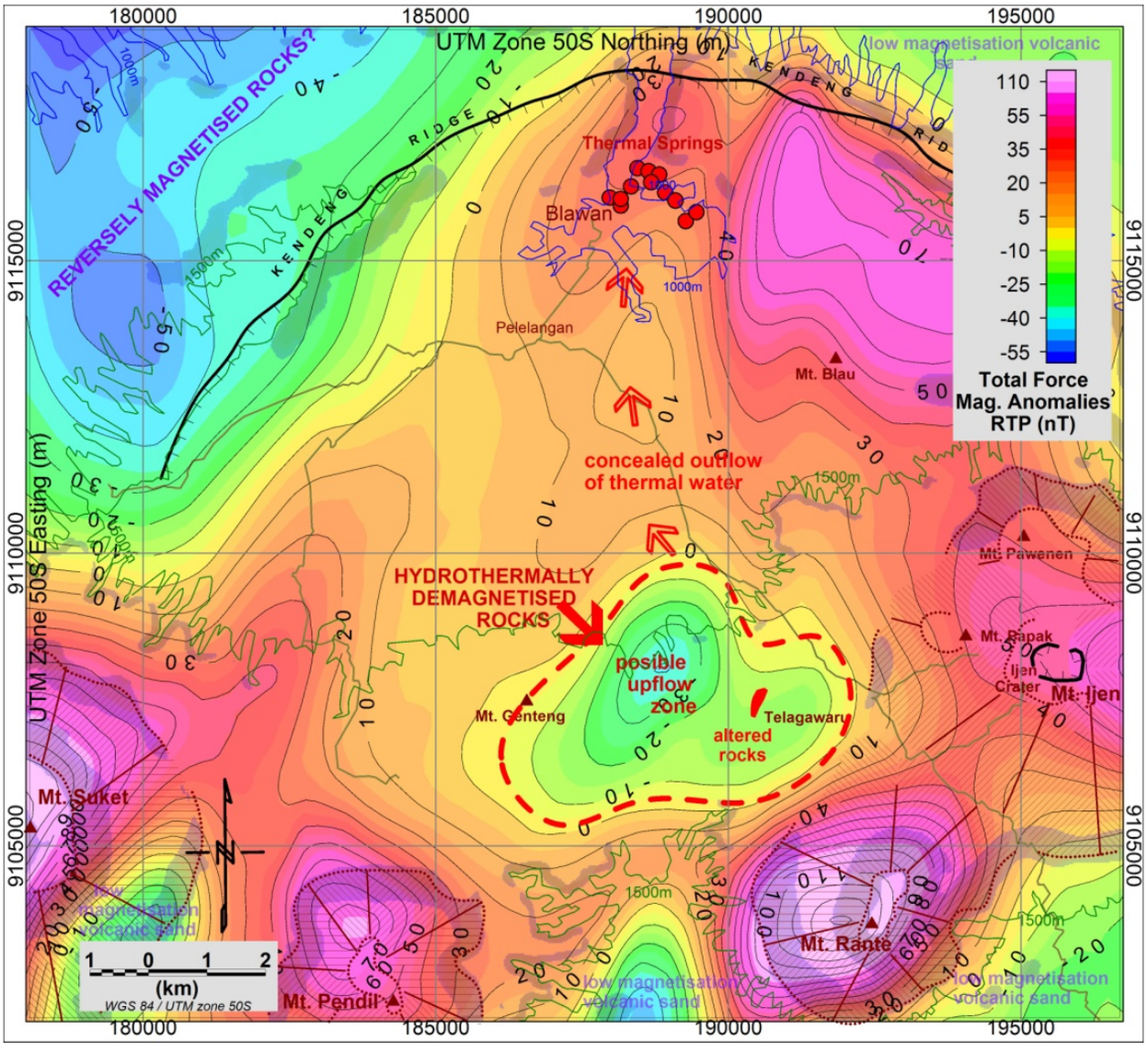

Figure 21. The result of reduction to pole (RTP) of the total force magnetic anomalies (ΔF) over the Ijen geothermal field in the eastern Java (Indonesia).

anomalies. This confusion can be eliminated by passing the measured total force magnetic anomalies (gridded at regular spacing) through the reduction to pole (RTP) transformation. Any anomalies caused by demagnetised reservoir will become dominantly negative. Furthermore, the lateral extent of the negative RTP would approximate the lateral extent of the demagnetised reservoir, so the magnetic RTP data can help delineate the geothermal reservoir. Special care must be taken, however, when working close (within about ±10°latitude) to the magnetic equator, that the software used to perform the RTP transform can run properly for data from low magnetic inclination regions. In general, the farther away the location is from the magnetic equator, the easier it is to delineate the source body from the total force magnetic anomalies.

The occurrence of reversely magnetised rocks can make interpretation of airborne magnetic data for geothermal reservoir becomes more difficult. The reversely magnetised rocks have a similar effect in the airborne magnetic map as the hydrothermally demagnetised rocks. The two can be distinguished from each other only when they occur in prominent topography. Hydrothermally demagnetised rocks will cause no specific total magnetic anomalies whereas the reversely magnetised rocks will appear as negative total force magnetic anomalies over the topography. In any other circumstances it is difficult to distinguish the two from magnetic anomaly map alone. As shown in the examples in Section 5, a geological interpretation is needed to resolve the problem.

The discussions presented in this chapter should equip readers with a sufficient knowledge to confidently organise and run airborne magnetic investigation of high temperature geothermal reservoirs in volcanic setting. The three examples on real airborne magnetic surveys given in the Section 5 could be used as reference for most cases of airborne magnetic investigations of geothermal resources.

Author details

Supri Soengkono*

Address all correspondence to: s.soengkono@gns.cri.nz

GNS Science, Wairakei Research Centre, Taupo, NewZealand

References

[1] Baranov, V.. A new method for interpretation of aeromagnetic maps: Pseudo-gravimetric anomalies: Geophysics. 1957; 22: 359–383.

[2] Barnett C.T.. Theoretical modelling of the magnetic and gravitational fields of an shaped three-dimensional body. Geophysics. 1976; 41(6):175-196.

[3] Dobrin M.B. and Savit C.H.. Introduction to Geophysical Prospecting. McGraw Hill International Editions; 1988. 876 p.

[4] Bohnsack, G.. The Solubility of Magnetite in Water and in Aqueous Solutions of Acid and Alkali. Hemisphere, Washington, D.C.; 1987. 161 pp.

[5] Browne, P. R. L. and Ellis, J. A.. The Ohaaki-Broadlands hydrothermal area, New Zealand: mineralogy and related geochemistry. American Journal of Science. 1970; 269: 97-131.

[6] Butler, R. F.. Paleomagnetism: Magnetic Domains to Geologic Terranes. BlackwellScientific, Boston, M.A.; 1992. 319 p.

[7] Dobrin M.B. and Savit C.H.. Introduction to geophysical prospecting. 4th ed. 1988: McGraw-Hill International Editions; 1988. 876 p.

[8] Ewart, A.. Review of mineralogy and chemistry of the acidic rocks of TaupoVolcanic Zone, New Zealand. Bulletin Volcanologique. 1966; 29: 147-172.

[9] Gerard, V. B. and Lawrie, J. A.. Aeromagnetic surveys in New Zealand, 1949-1952. Geophysical Memoir 3, Department of Scientific and Industrial Research, Wellington, New Zealand; 1955.

[10] Grindley, G. W., Mumme, T. C. and Kohn, B. P.. Stratigraphy, paleomagnetism, geochronology and structure of silicic volcanic rocks, Waiotapu/Paeroa Range area, New Zealand. Geothermics. 1994; 23:473-499.

[11] Hedenquist, J. W. and Stewart, M. K.. Natural CO2-rich steam-heated waters in the Broadlands-Ohaaki geothermal system, New Zealand. Geothermal Resources Council Transactions. 1985; 9: 245-250.

[12] Henrys, S. A. and van Dijck, M. F. (1987) Structure of concealed rhyolites and dacites in the Broadlands-Ohaaki geothermal field. NZ Geothermal Workshop Proceedings. 1987; 9: 43-48.

[13] Henrys, S. A. and Hochstein, M. P.. Geophysical structure of Broadlands-Ohaaki geothermal field (New Zealand). Geothermics. 1990; 19: 129-150.

[14] Hochstein, M.P and Soengkono, S.: Magnetic anomalies associated with high temperature reservoirs in the Taupo Volcanic Zone (New Zealand). Geothermics. 1997; 26: p 1-24.

[15] Hunt, T.M., Bromley, C.J., Risk, G.F. and Soengkono, S.: Geophysical investigation of the Wairakei field. Geothermics. 2009; 38: 85-97.

[16] Hunt, T. M. and Whiteford, C. M.. Sheet 5, Rotorua. Magnetic map of New Zealand 1:250000, Total Force Anomalies. DSIR, Wellington, New Zealand. 1979.

[17] Lawton, D. C. and Hochstein, M. P. (1980) Physical properties of titanomagnetite sands. Geophysics. 1980; 45:394-402.

[18] Li, Y. and Oldenburg, D. W.. Stable reduction to the pole at the magnetic equator. Geophysics. 2001; 66(2): 571-578.

[19] Mankinen, E.A. and Dalrymple, G.B. (1979) Revised magnetic polarity time scale for the interval 0-5 m.y. BP. Journal of Geophysical Research. 1979; 85: 615-626.

[20] Soengkono, S. (1985) Magnetic study of the Mokai geothermal field. NZ Geothermal Workshop Proceedings. 1985; 7: 25-30.

[21] Soengkono, S.. Geophysical studies of the Western Taupo Volcanic Zone. PhD. thesis, The University of Auckland. 1990:350 p.

[22] Soengkono, S.: Magnetic anomalies over the Ngatamariki geothermal field. NZ Geothermal Workshop Proceedings. 1992; 14: 241-246.

[23] Soengkono, S. (1993) Interpretation of aeromagnetic data over the Orakeikorako geothermal field, Central North Island, New Zealand. NZ Geothermal Workshop Proceedings. 1993; 15: 207-212.

[24] Soengkono, S. (1995) A magnetic model for deep plutonic bodies beneath the central Taupo Volcanic Zone, North Island, New Zealand. Journal of Volcanology and Geothermal Research. 1995; 68: 193-207.

[25] Soengkono, S.: Interpretation of magnetic anomalies over the Waimanggu geothermal area, Geothermics. 2001;30: 443-459.

[26] Soengkono, S., Hochstein, M.P. and van Dijk, M.F.: Magnetic anomalies of the Rotokawa geothermal field, Taupo Volcanic Zone. NZ Geothermal Workshop Proceedings. 1991; 13: 33-38.

[27] Soengkono, S. and Hochstein, M. P.: Magnetic anomalies over the Wairakei geothermal field, central North Island, New Zealand. Geothermal Resources Council Transactions. 1992; 16: 273-278.

[28] Soengkono, S., Hochstein, M.P, Smith, I. E. M. and Itaya, T.: Geophysical evidence for widespread reversely magnetized pyroclastics in the western Taupo Volcanic Zone (New Zealand), NZ Journal of Geology and Geophysics. 1992; 35: p 47-55.

[29] Soengkono, S. and Hochstein, M. P. (1995) Application of magnetic method to assess the extent of high temperature geothermal reservoirs. Proceedings 20th Workshop Geothermal Reservoir Engineering Proceedings, Stanford University, CA. 1996; 20:71-78.

[30] Soengkono, S. and Hochstein, M. P. (1996) Preliminary interpretation of magnetic anomalies over the Waimangu, Waiotapu, Waikite and Reporoa geothermal areas, New Zealand. PNOC-EDC Geothermal Conference Proceedings. 1996; 17: 197-203.

[31] Soengkono, S.; Henderson, S.; Hungerford, N.; Doyle, S.; Cottin, E.. Ultra-detailed airborne geophysical surveys applied in an integrated approach to gold exploration in New Zealand. Preview / Australian Society of Exploration Geophysicists. 2007; 129: 14-17

[32] Steiner, A. (1953) Hydrothermal rock alteration at Wairakei, New Zealand. Economic Geology. 1953; 48: 1-13.

[33] Steiner, A. (1977) The Wairakei Geothermal Area, North Island, New Zealand. NZ Geological Survey Bulletin, DSIR, Wellington. 1977; 90: 1-13.

[34] Swain C, 2000 Reduction to the pole of regional magnetic data with variable field direction and its stabilisation at the low inclinations. Exploration Geophysics. 2000; 31: 78-83.

[35] Watson-Munro, C. N. (1938) Reconnaissance survey of the variation of magnetic force in the New Zealand thermal regions. NZ Journal of Science and Technology. 1938; B20: 99-115.

[36] Whiteford, C. M.. Magnetic anomaly map of Central Volcanic region. Geophysics Division, DSIR, Wellington. 1979; Report 101.

IntechOpen